ISTANBUL TECHNICAL UNIVERSITY ★ GRADUATE SCHOOL OF SCIENCE ENGINEERING AND TECHNOLOGY

SURFACE MODIFICATION OF TITANIUM SUBSTRATES WITH NANO HYDROXYAPATITE COATED CHITOSAN MICROSPHERES

M.Sc. THESIS

Burcu DOYMUŞ

Department of Molecular Biology-Genetics and Biotechnology

Molecular Biology-Genetics and Biotechnology Programme

JULY 2020

ISTANBUL TECHNICAL UNIVERSITY ★ GRADUATE SCHOOL OF SCIENCE ENGINEERING AND TECHNOLOGY

SURFACE MODIFICATION OF TITANIUM SUBSTRATES WITH NANO HYDROXYAPATITE COATED CHITOSAN MICROSPHERES

M.Sc. THESIS

Burcu DOYMUŞ
(521171102)

Department of Molecular Biology-Genetics and Biotechnology

Molecular Biology-Genetics and Biotechnology Programme

Thesis Advisor: Prof. Dr. Fatma Neşe KÖK
Thesis Co-Advisor: Dr. Sakip ÖNDER

JULY 2020

ISTANBUL TEKNİK ÜNİVERSİTESİ ★ FEN BİLİMLERİ ENSTİTÜSÜ

NANO HİDROKSİAPATİT KAPLI KİTOSAN MİKROKÜRELER İLE TİTANYUM MALZEME YÜZEYLERİNİN DEĞİŞTİRİLMESİ

YÜKSEK LİSANS TEZİ

Burcu DOYMUŞ
(521171102)

Moleküler Biyoloji-Genetik ve Biyoteknoloji Anabilim Dalı

Moleküler Biyoloji-Genetik ve Biyoteknoloji Programı

Tez Danışmanı: Prof. Dr. Fatma Neşe KÖK
Eş Danışman: Dr. Sakip ÖNDER

TEMMUZ 2020

Burcu DOYMUŞ, a M.Sc. student of İTU Graduate School of Science Engineering and Technology student ID 521171102, successfully defended the thesis entitled "SURFACE MODIFICATION OF TITANIUM SUBSTRATES WITH NANO HYDROXYAPATITE COATED CHITOSAN MICROSPHERES", which she prepared after fulfilling the requirements specified in the associated legislations, before the jury whose signatures are below.

Thesis Advisor :	**Prof. Dr. Fatma Neşe KÖK** Istanbul Technical University	.....
Co-advisor :	**Dr. Sakip ÖNDER** Yıldız Technical University	.....
Jury Members :	**Prof. Dr. Ayten KARATAŞ** Istanbul Technical University	.....
	Prof. Dr. Muhammet Kürşat KAZMANLI Istanbul Technical University	.....
	Dr. Timuçin AVŞAR Bahcesehir University	.....

Date of Submission : 15 June 2020
Date of Defense : 16 July 2020

To my family,

FOREWORD

First of all, I would like to thank my supervisor Prof. Dr. Fatma Neşe Kök for her advice, encouragement and support during this study. I am grateful for her patience and understanding. I would like to express my special thanks to my co-supervisor Dr. Sakip Önder for his support, encouragement and guidance. His advice and comments were very important for me.

I would like to thank Erkan Kaçar for his help in EDS, SEM and XRD analysis. I am also thankful to Dr. Barbaros Akkurt and Prof. Dr. Ahmet Gül for their help in FTIR analysis.

I would like to thank my labmates, Ayşe Buse Özdabak, Gizem Kerem, Canan Çil, Elifcan Zengin, Yeliz Erşan, Ceren Kutlu Kaya and Şebnem Seherler for their wonderful cooperation and friendship. They always kept me motivated. Their supports were very important for me. A special thanks to Ayşe Buse Özdabak who always answered my questions and helped me for laboratory works.

I would like to express my appreciation to my family, my mother Güler, my father Mustafa Kemal and my brothers Arif and Özgür for their support and love.

I would also like to acknowledge the TUBITAK Project (217M220) for financial support.

July 2020 Burcu DOYMUŞ

TABLE OF CONTENTS

Page

FOREWORD ..... **ix**
TABLE OF CONTENTS ..... **xi**
ABBREVIATIONS ..... **xiii**
SYMBOLS ..... **xv**
LIST OF FIGURES ..... **xvii**
SUMMARY ..... **xix**
ÖZET…… ..... **xxi**
1. INTRODUCTION **1**
1.1 Purpose of Thesis 1
1.2 Metallic Biomaterials 1
1.2.1 Titanium and its alloys 2
1.2.2 Nano hydroxyapatite (nHA) 3
1.3 Implant Associated Infections 4
1.4 Controlled Drug Delivery 6
1.4.1 Chitosan 7
1.4.2 Microspheres as drug carriers 9
1.4.3 Ciprofloaxacin 10
2. MATERIALS AND METHODS **11**
2.1 Materials 11
2.2 Methods 11
2.2.1 Synthesis of the chitosan microspheres 11
2.2.2 Size analysis of microspheres 12
2.2.3 Preparation and characterization of titanium surfaces 12
2.2.3.1 Surface modification of titanium plates 12
2.2.3.2 Immobilization of microspheres 13
2.2.3.3 Nano hydroxyapatite (nHA) coating 13
2.2.3.4 Characterization of titanium surfaces 14
2.2.4 Drug release studies 14
3. RESULTS AND DISCUSSION **15**
3.1 Sizes of Chitosan Microspheres 15
3.2 Characterization of Surface Modified Titanium Plates 17
3.3 Optimization of Microsphere Immobilization 19
3.4 Effects of Immobilization on Drug Release 23
3.5 Characterization of Nano Hydroxyapatite Coatings 24
3.5.1 FTIR analysis 24
3.5.2 SEM and EDS analysis 25
3.5.3 XRD analysis 29
3.6 Stability of Whole System 30
3.7 Effects of Nano Hydroxyapatite Coatings on Drug Release 31
4. CONCLUSIONS AND RECOMMENDATIONS **35**

REFERENCES **37**
APPENDICES **43**
CURRICULUM VITAE **45**

ABBREVIATIONS

APTES **:** 3-Triethoxysilylpropylamine
EDS **:** Energy Dispersive X-ray Spectroscopy
FT-IR **:** Fourier Transform Infrared Spectroscopy
GA **:** Glutaraldehyde
nHA **:** Nano hydroxyapatite
PBS **:** Phosphate-buffered saline
rpm **:** Revolutions per minute
SEM **:** Scanning Electron Microscopy
Ti **:** Titanium
XRD **:** X-Ray Diffractometer

SYMBOLS

cm^2	**:** square centimeter
g	**:** gram
ml	**:** milliliter
mM	**:** milli molar
nm	**:** nanometer
µg	**:** microgram
µl	**:** microliter

LIST OF FIGURES

Page

Figure 2.1 : Schematic representation of drug loaded microsphere synthesis. 12
Figure 2.2 : Schematic representation of surface modification of titanium plates. .. 13
Figure 2.3 : Schematic representation of microsphere immobilization on titanium plates. 13
Figure 2.4 : Schematic representation of nano hydroxyapatite coating. 14
Figure 3.1 : Light microscope images (10x) of microspheres prepared at **a)** 300 rpm **b)** 400 rpm and **c)** 500 rpm stirring rate 15
Figure 3.2 : Size distribution of the microspheres prepared at different stirring rates. 16
Figure 3.3 : SEM micrographs of microspheres prepared at 500 rpm at **a)** 200x and **b)** 4000x **c)** 6000x..... 17
Figure 3.4 : SEM micrographs of Ti surfaces (10.000x) **a)** polished **b)** alkali treated **c)** silanized 18
Figure 3.5 : FT-IR spectra of alkali treated and silanized Ti surfaces. 19
Figure 3.6 : SEM micrograph of the Ti surface coated with mixture of 100 µl chitosan solution and 5 mg microsphere (100:5, µl:mg) **a)** (200x) and **b)** (1000x)..... 20
Figure 3.7 : SEM micrograph of the Ti surface coated with mixture of 50 µl chitosan solution and 10 mg microsphere (50:10, µl:mg). **a)** fructures of chitosan film (100x) and **b)** flaking of microspheres (100x) 20
Figure 3.8 : SEM micrograph of the surface coated with mixture of 50 µl chitosan solution and 5 mg microsphere (50:5, µl:mg). **a)** (49x) and **b)** (108x). 21
Figure 3.9 : SEM micrographs of 3 different samples (prepared with ratio of 50:5 (µl:mg)) **(a,b) (c,d)** and **(e,f)** at different magnifications:100x **(a,c,e)** and 300x **(b, d, f)**. 22
Figure 3.10 : Overall cumulative release of ciprofloxacin from free and immobilized microspheres. 23
Figure 3.11 : Percentage cumulative release of ciprofloxacin from free and immobilized microspheres for 24 h. 24
Figure 3.12 : FT-IR spectra of uncoated and nHA coated microspheres. 25
Figure 3.13 : SEM micrographs of nHA coated microspheres **a)**10.000x and **b)**15.000x. 25
Figure 3.14 : EDS analysis of nHA coated microsphere (10.000x). 26
Figure 3.15 : SEM micrographs of chitosan sponges **a)** uncoated **b)** nHA coated (1000x)..... 27
Figure 3.16 : EDS analysis of nHA coated chitosan sponge (3500x). 27
Figure 3.17 : SEM micrographs of nHA coated microsphere-chitosan modified Ti surfaces (3500x). 28
Figure 3.18 : EDS analysis of nHA coated Ti surface. 29

Figure 3.19 : XRD patterns of **a)** uncoated **b)** nHA coated chitosan-microsphere modified Ti surfaces. 30
Figure 3.20 : SEM micrographs of nHA coated microsphere-chitosan modified Ti surfaces after keeping in PBS (30 days). 31
Figure 3.21 : Overall cumulative release of ciprofloxacin from nHA coated and uncoated immobilized microspheres..... 32
Figure 3.22 : Percentage cumulative release of ciprofloxacin from nHA coated and uncoated immobilized microspheres for 24 h. 33

SURFACE MODIFICATION OF TITANIUM SUBSTRATES WITH NANO HYDROXYAPATITE COATED CHITOSAN MICROSPHERES

SUMMARY

Today, implants are increasingly used to replace or support the damaged structure or function in human body. Titanium and Ti based materials are commonly preferred as implant materials due to their superior mechanical features and biocompatibility. Although implants are biocompatible, well designed, and functional, they carry the risk of infection. Implant associated infections are serious problem after surgical operations because they generally lead to revision surgery and thus increase morbidity, length of hospitalization and health care cost. These infections are generally caused by the attachment of microorganisms to the implant surface and subsequently biofilm formation. In order to address this problem, surface modification of implant materials and drug delivery strategies have been studied. Releasing antibiotics from the implant surfaces is an effective approach to increase the implant success by local antimicrobial delivery. For further improvement, the hydroxyapatite coating is one of the most preferred methods to fasten osseointegration.

In this study, Ti surfaces were modified with antibiotic loaded chitosan microspheres and coated with nano hydroxyapatite (nHA) to prevent implant related infections and increase the osseointegration. Firstly, antibiotic (ciprofloxacin) loaded chitosan microspheres were prepared via emulsion/cross-linking method using different stirring rates (300, 400 and 500 rpm) and analyzed under light and electron microscopes. It was seen that more homogenous size distribution and smaller microspheres were obtained with increasing stirring rate and 500 rpm was preferred for microsphere production. Before the immobilization of microspheres, Ti plates were oxidized and then silanized with APTES (3-Triethoxysilylpropylamine) to form amino groups ($-NH_2$) on the surfaces. Ti plates were characterized with Fourier transform infrared spectroscopy (FT-IR) to analyze the chemical composition of surfaces and scanning electron microscopy (SEM) to examine surface morphology. Characterization studies proved that chemical groups required for cross-linking were formed on the surfaces. After that, the chitosan solution was used for immobilization of the microspheres. Microsphere - chitosan solution (2%) was prepared and spread on Ti surfaces activated with glutaraldehyde GA (8%) for cross-linking, then the samples were freeze-dried and analyzed by SEM. The amount of chitosan solution and microspheres were optimized, and the chitosan to microsphere ratio was chosen as 50:5 (µl:mg) for 1.5 cm^2 Ti plate. Secondly, microsphere – chitosan modified Ti samples were coated with nHA using $CaCl_2$ (1.25 mM) and Na_2HPO_4 (0.75 mM) solutions. The presence of nHA was analyzed with FT-IR and X-ray diffraction spectroscopy (EDS), and the crystalline structure of nHA was analyzed with an X-Ray diffractometer (XRD) then nHA structures on the surfaces were viewed by SEM. Characteristic functional groups (-OH and $-PO_4^{-3}$) of nHA were detected in FT-IR analysis and Ca and P minerals were observed in EDS analysis. Before the drug release study, the whole system was tested

in PBS for 30 day and flaking or fractures were not observed showing the stability of the system. Finally, drug release studies were carried out with free and immobilized microspheres (uncoated and nHA coated) and it was seen that sufficient amount of drug can be released from Ti surfaces although drug release profiles were affected by immobilization and nHA coating. Thus, a dual-functional system with antibacterial activity and tissue integration ability could be made. This system will be used in animal experiments after the antibacterial and bioactivity studies.

NANO HİDROKSİAPATİT KAPLI KİTOSAN MİKROKÜRELER İLE TİTANYUM MALZEME YÜZEYLERİNİN DEĞİŞTİRİLMESİ

ÖZET

Günümüzde teknolojideki gelişmelerle birlikte insan vücudundaki eksik veya hasarlı yapıları onarmak için yapılan implant tedavileri de artmaktadır. İnsan vücudundaki kemik ve eklemlerde işlev kaybı, zayıflama ve iltihaplanma gibi sağlık problemlerinin çok olmasından dolayı kalça, diz ve spinal protez ameliyatları en sık yapılan implant tedavileridir. Bu gibi sert doku tedavilerinde titanyum ve alaşımlarından üretilen implant malzemeleri, biyouyumlulukları ve geliştirilebilir mekanik özellikleri nedeniyle sıkça kullanılmaktadır. İmplantlar biyouyumlu, iyi tasarlanmış fonksiyonel malzemeler olsalar bile yüksek enfeksiyon riski taşımaktadırlar. İmplantla ilişkili enfeksiyonlar genellikle ameliyatların tekrarlanmasıyla tedavi edildikleri için morbidite oranını, hastanede yatış süresini ve sağlık masraflarını artırmaktadırlar. Bu nedenle implanttan kaynaklanan enfeksiyonlar, cerrahi işlemler sonrasında karşılaşılan en büyük problemlerden biridir. İmplantla ilgili enfeksiyonları önlemek ve kemik-doku etkileşimini artırmak için implant yüzeylerinin işlevselleştirilmesi ve ilaç salımı ile ilgili çalışmalar yapıldığı görülmektedir.

İmplanla ilişkili enfeksiyonları önlemek için antimikrobiyal implant yüzeyleri hazırlamak en önemli yaklaşımlardan biridir. Bu yüzeyler ya mikroorganizmaların yüzeye tutunmasını engelleyecek yada yüzeyden biyosit salımı yapılarak öldürülmesini sağlayacak kaplamalarla hazırlanmaktadır. Bölgesel ajan salımı yapan sistemlerin uzun süreli kullanım için daha etkili oldukları görülmüştür. Bu nedenle dirençli mikroorganizmaların yüzeye bağlanması ve sonrasında biyofilm oluşturmasıyla oluşan bu enfeksiyonlarla mücadele etmek için, yüzeylerinden antimikrobiyal ajan salımı yapabilen sistemler üzerine araştırmalar yoğunlaşmıştır.

İlaç salım sistemlerinde, mikro küre temelli sistemler özel uygulama alanları sağladığı, biyoyararlanımı artırdığı, uzun süreli terapötik etki sağladığı, kullanılan dozu ve toksik etkiyi azalttığı ve kontrollü salımı sağladığı için sıkça kullanılır. Mikroküre esaslı ilaç salım sistemlerinde, biyouyumlu, biyolojik olarak bozunabilen ve toksik olmayan kitosan, sıkça tercih edilen doğal polimerlerden biridir. Bu çalışmada da ilacın kontrollü salımı için kitosan esaslı mikro kürelerle çalışılmıştır.

İmplant malzemesinin yüzey özelliklerini geliştirmek böylece implant/doku arakesitinde hızlı ve kuvvetli bağlar oluşturmak için nano hidroksiapatit (nHA) kaplamalar yaygın olarak kullanılmaktadır. Yapılan çalışmalarda, nano hidroksiapatit kaplamalarının kemik hücrelerinin çoğalmasını artırdığı, çekirdeklenme merkezi oluşturarak apatit çökelmesini hızlandırdığı ve antimikrobiyal etkisinin olduğu görülmektedir. Hücreler üzerindeki olumlu etkileri ve antimikrobiyal özellikleri nedeniyle bu çalışmada nHA kaplama kullanılmıştır.

Bu çalışmanın amacı, implantla ilişkili enfeksiyonları önlemek ve osseoentegrasyonu arttırmak için titanyum yüzeylerinin değiştirilmesidir. Bu amaçla titanyum (Ti)

yüzeyler antibiyotik yüklü kitosan mikroküreler ile modifiye edilmiş ve nano hidroksiapatit ile kaplanmıştır. İlk olarak, antibiyotik (siprofloksasin) yüklü kitosan mikroküreler emülsiyon çapraz bağlama yöntemi kullanılarak üretilmiştir. Karıştırma hızının mikroküreler üzerindeki etkisini incelemek için farklı karıştırma hızları (300, 400 ve 500 rpm) kullanılmıştır. Üretilen kürelerin boyutları ve morfolojileri ışık ve elektron mikroskopları kullanılarak analiz edilmiştir. Karıştırma hızının artmasıyla birlikte küre boyutlarının küçüldüğü ve daha homojen bir boyut dağılımı elde edildiği görülmüştür, bu nedenle küreler 500 rpm karıştırma hızı kullanılarak üretilmiştir. Mikroküreler yüzeye tutuklanmadan önce titanyumun yüzeyler aktifleştirilmiştir. Öncelikle titanium plaka 1,5 cm^2 boyutlarında kesilmiştir ve hazırlanan yüzeyler kimyasal olarak parlatılmıştır. Parlatılan titanyum altlık malzemeler, yüzeylerinde hidroksil gruplarının (-OH) oluşması amacıyla alkali işlem uygulanarak oksitlenmiştir. Sonrasında yüzeylerde çapraz bağlanma için gerekli olan amino gruplarının ($-NH_2$) oluşması için APTES (3-Trietoksisililpropilamin) ile silanize edilmiştir. Ti altlık malzeme yüzeylerinde oluşan kimyasal grupları analiz etmek için Fourier dönüşümlü kızılötesi spektroskopisi (FT-IR) ve yüzey morfolojisini incelemek için taramalı elektron mikroskobu (SEM) kullanılmıştır. FT-IR analizinde, oksitlenen yüzeylerde -OH grupları ve silanlanan yüzeylerde $-NH_2$ grupları tespit edilmiştir. SEM analizinde, oksitlenen yüzeylerde ağsı yapıların oluştuğu görülürken silanlandıktan sonra ağsı yapıların kaybolduğu daha yoğun bir tabaka oluştuğu görülmüştür. Yüzeylerin çapraz bağlanma için hazır olduğu görüldükten sonra, hazırlanan mikroküreler bu yüzeylere kitosanın serbest amino grupları kullanılarak immobilize edilmiştir. Bunun için, kitosan solüsyonu (%2)-mikroküre karışımı hazırlanmıştır. Daha sonra, son olarak silanlanmış olan yüzeyler gluteraldehit (GA, %8) ile aktifleştirilerek çapraz bağlanma için hazır hale getirilmiştir. Kitosan solüsyonu-mikroküre karışımı aktive edilen Ti yüzeylere ince bir tabaka halinde yayılmıştır ve hazırlanan titanyum numuneler liyofilizasyon işlemiyle kurutulmuştur. Kurutulan numuneler yüzeydeki kaplamanın incelenmesi amacıyla elektron mikroskobu ile analiz edilmiştir. Kitosan solüsyonu : mikroküre (µl:mg) oranı 100:5, 50:10 ve 50:5 oranları kullanılarak optimize edilmiştir. Mikrokürelerin yüzeyden ayrılmadığı ve kitosan filmin kırılmadığı yani kaplamanın stabil ve homojen olduğu 50:5 (µl:mg) kitosan solüsyonu : mikroküre oranı, 1,5 cm^2 boyutundaki bir Ti plaka için optimum olarak belirlenmiştir ve ilerleyen çalışmalarda bu oran kullanılmıştır. İkinci olarak, kitosan film yardımıyla mikroküre immobilize edilen Ti yüzeyler çöktürme yöntemi kullanılarak nano hidroksiapatit (nHA) ile kaplanmıştır. Bunun için kitosana ait amino gruplarıyla koordine kovalent bağa ile ve ayrıca hidroksil gruplarıyla elektrostatik etkileşime dayanan çöktürme işlemi gerçekleştirilmiştir. Bu amaçla öncelikle $CaCl_2$ (1.25 mM) kalsiyum kaynağı olarak kullanılmıştır. Kalsiyumun yüzeyde birikmeye başlamasından sonra, Na_2HPO_4 (0.75 mM) solüsyonu fosfat kaynağı olarak kullanılarak nHA çökelmesi gerçekleştirilmiştir. Yüzeylerdeki nHA varlığı FT-IR ve X-ışını kırınım spektroskopisi (EDS) ile analiz edilmiştir. Kristal yapısı X ışını kristalografisi (XRD) ile analiz edilmiştir ve morfolojik yapısı SEM ile görüntülenmiştir. FT-IR analizinde, nHA yapısına ait karakteristik fonksiyonel gruplar (-OH ve $-PO_4^{-3}$) ve EDS analizinde, Ca ve P minerallerinin varlığı gözlemlenmiştir. İlaç salım çalışmasından önce, mikroküre immobilize edilen ve nHA ile kaplanan Ti yüzeyler 30 gün boyunca PBS içinde bekletilerek test edilmiştir ve yüzeylerde bozulma veya mikrokürelerin kopması gibi olumsuzluklar gözlemlenmemiştir. Sistemin stabil olduğunun tespit edilmesinden sonra, ilaç salım çalışmaları serbest ve immobilize edilmiş mikroküreler (kaplanmamış ve nHA kaplanmış) ile gerçekleştirilmiştir. İmmobilizasyon işleminin ve nHA

kaplamanın ilaç salım hızını yavaşlattığı gözlemlenmiştir. Buna rağmen tüm yüzeylerden sürekli ve yeterli ilaç salımı yapılabildiği görülmüştür.

Böylece antimikrobiyal etki ve hızlı osteoentegrasyon yeteneği gibi iki fonksiyonalitesi olan sistem yapılabilmiştir. Bu sistem, antimikrobiyal aktivite ve biyoaktivite testlerinden sonra hayvan deneylerine uygulanabilecektir.

1. INTRODUCTION

1.1 Purpose of Thesis

Implant related infections are an important factor affecting the success of implant materials. These infections cause the prolonged hospitalization, a painful recovery process, and even cause the removing implant. Surface properties of the implant are another important factor affecting the success of the implant materials. Therefore, the surfaces of the implant materials are changed by applying different processes to improve osseointegration. Antimicrobial agent release and nano hydroxyapatite coating are important approaches to improve the properties of the implant materials. The aims of this study, it is to change the surface of titanium materials to prevent implant associated infections while increasing the implant – tissue integration. For this purpose, antibiotic loaded chitosan microspheres were attached to Ti surfaces and nano hydroxyapatite was synthesized on these surfaces.

1.2 Metallic Biomaterials

Biomaterials are biological or synthetic materials that are used in medical tools or interact with living tissues to replace or assist damaged tissue or organs without any adverse effects (Ghasemi-Mobarakeh et al., 2019). Biomaterials are grouped into three main types as metallic, ceramic and polymeric materials. Also, there were composites, which are combinations of two or more materials (Williams, 2009). Metallic biomaterials are generally used in hard tissue applications such as bone and dental implants (Figure 1.1) because of their mechanical performance. Metallic biomaterials can be categorized according to their major element: stainless steels, cobalt alloys, and titanium and its alloys. Biocompatibility, suitable mechanical features, high corrosion and wear resistance, and osseointegration ability are the main requirement of metallic biomaterials (Chen & Thouas, 2015). Biocompatibility is the physical, chemical, biological compatibility of a material to body tissues and the optimum adaptation to

the body mechanism. Also, osseointegration is the integration ability between bone and surface of implanted material (Ghasemi-Mobarakeh et al., 2019).

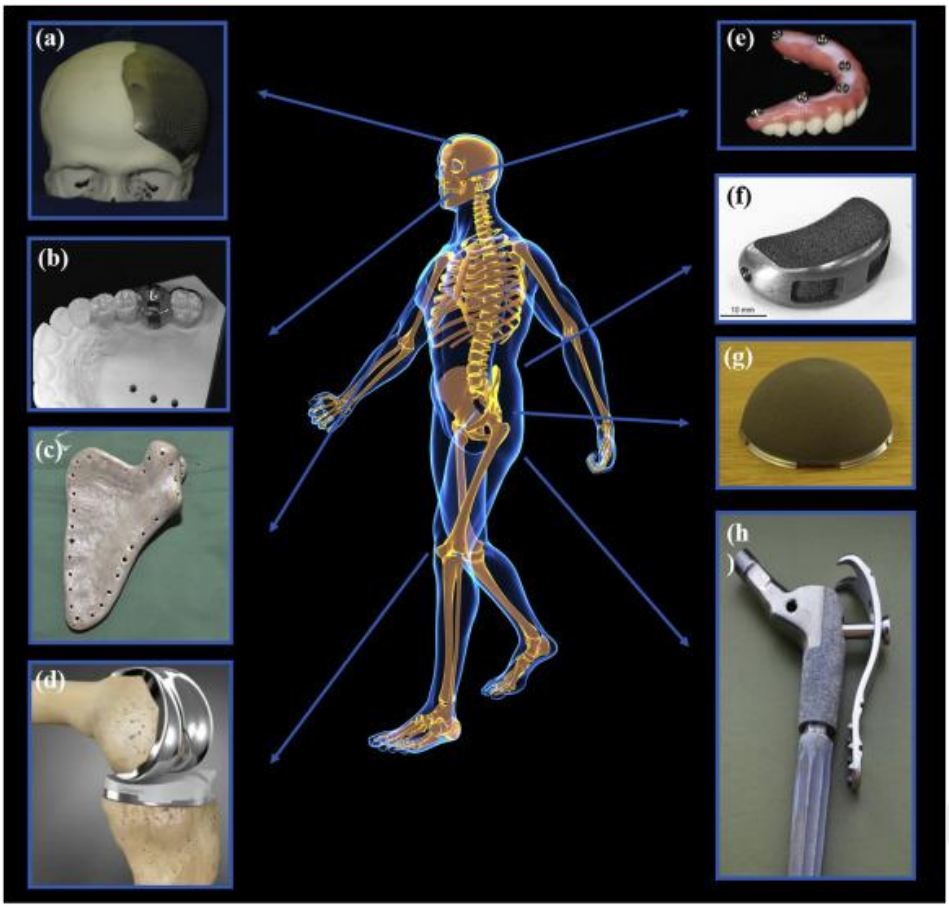

Figure 1.1 : The medical application of metal biomaterials (Ni et al., 2019).

1.2.1 Titanium and its alloys

Titanium and Ti-based materials are commonly preferred in biomedical applications because of their high biocompatibility, high corrosion resistance, low density and low elastic modulus. Although Ti based materials have these excellent features, they are weak in terms of wear resistance. Also, elasticity of these materials is much closer to bone when compared to stainless steels and cobalt alloys, so they are generally used in dental and orthopedic prostheses as replacement parts or fixation elements (Kaur & Singh, 2019; Manivasagam et al., 2010). The most employed titanium materials are commercially pure Ti and Ti–6Al–4V. Alloys without vanadium have been developed for medical usage since vanadium is found to be toxic (Kaur & Singh, 2019). Titanium materials are inert and do not interact with the surrounding tissues when they are implanted. Although, when a bio-inert device is implanted, the body's defense

mechanism responses to implant (Figure 1.2) and this system causes permanent implants to loosen, titanium implants show close integration with the host bone tissue. Only Ti materials are capable to connect with bone among metallic materials (Chen & Thouas, 2015).

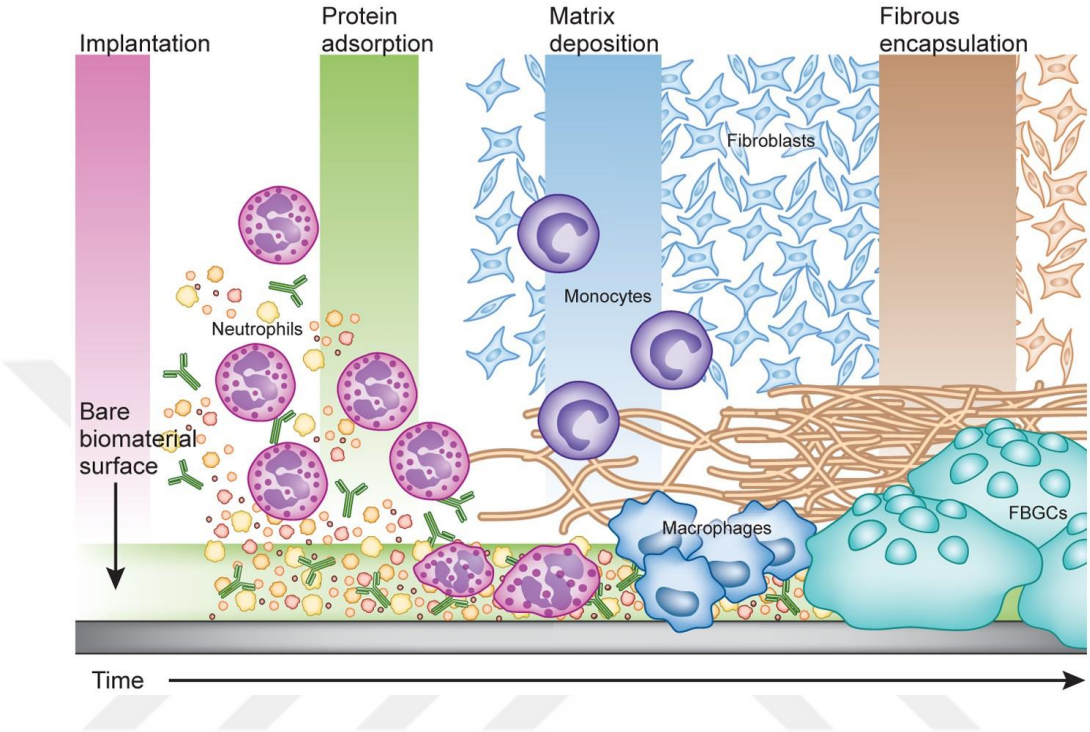

Figure 1.2 : Representation of host response to biomaterial after implantation (Grainger, 2013).

Surface modifications like heat treatment, ion deposition or chemical treatment are used to improve the bioactivity or mechanical properties of titanium materials. Hydroxyapatite (HA) coatings are used to enhance the bone bonding ability of titanium implants (Kaur & Singh, 2019).

1.2.2 Nano hydroxyapatite (nHA)

Hydroxyapatite ($Ca_{10}(PO_4)_6(OH)_2$) is a ceramic material and contained in the structure of tooth enamel, dentin and bone. Synthetic HA is generally used in biomedical applications such as bone repair and bone regeneration as a composite with polymers or orthopedic and dental implants as a coating. The main reasons for its widespread use in medical applications are its great biocompatibility, similarity with bone mineral and excellent osteoconductive properties (Mali et al., 2016). It can form very strong bonds at the bone-implant interface and stimulate bone healing on this surface. Its

porous structure allows the cells to grow well and the tissues to penetrate into the implants. In addition, the pores in the structure of the HA act like the canals system, allowing the blood structure and other important body fluids to reach the bone structure (Sopyan et al., 2007). These ceramics cannot be used directly as hard tissue implants due to their high fragility. However, they can be used for improving the surface properties of metallic implants. Numerous methods such as plasma spraying method, pulsed laser deposition, electrophoretic deposition, sol-gel deposition and chemical deposition are used for deposition of HA on metallic materials (Ong & Chan, 2000).

Changing the surface properties of implant materials with nano hydroxyapatite (nHA) structures is also studied. Overall, performances of nanostructured biomaterials are much improved than their larger size equivalents due to the bigger surface / volume ratios and unusual effects. Nano sized HA has a higher surface roughness and smaller pore compared to micro-sized HA (Dorozhkin, 2010). Nano hydroxyapatite coatings have better bioactivity and osteointegration compared to conventional sized HA (Kim et al., 2005). In addition, nano sized HA increases apatite precipitation rate thus it accelerates the osseointegration (Kong et al., 2006).

1.3 Implant Associated Infections

Implant-related infection develops due to the bacterial adhesion on the implant surface and it is the serious complications related to the implant. This infection causes a high morbidity rate, prolonged hospitalization and recovery time, high hospital cost and revision surgery therefore it is a serious health problem. Contamination of a biomaterial can cause an infection that is hard to treat because of biofilm formation. (Moriarty et al., 2017). Biofilm is a community of microorganisms that attach to the surface and protect themselves with a polysaccharidic matrix they produce (Figure 1.3). Biofilms are highly resistant to body defense mechanisms and antibiotic treatments, therefore preventing attachment of bacteria is the important step of decreasing implant-associated infection risk (Ferraris & Spriano, 2016; Hetrick & Schoenfisch, 2006).

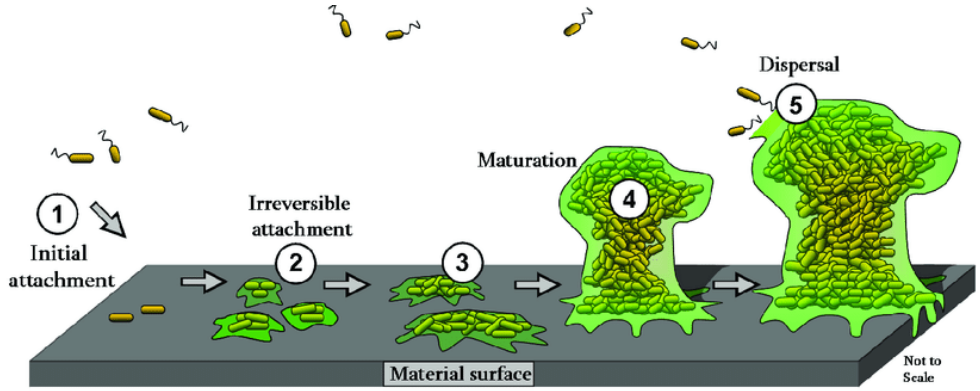

Figure 1.3 : Representation of biofilm formation on surface (Moriarty et al., 2017).

Gram-positive *Staphylococcus aureus* and *Staphylococcus epidermidis* are the most commonly detected pathogens that cause implant infections. *S. aureus* infections developed rapidly and are generally heavier compared to *S. epidermidis* infections. Other bacterias that cause infection are gram-negative *Escherichia coli and Pseudomonas aeruginosa* (Hetrick & Schoenfisch, 2006). Surface coating is the most important approach to prevent these infections. It can be divided into two groups as antifouling (Figure 1.4a) and antimicrobial (Figure 1.4b) coatings. Antifouling surfaces resist the bacterial accumulation by repulsive forces of immobilized polymer or structured surfaces and antimicrobial surfaces kill the bacteria by biocide releasing or direct contact (Kurtz & Schiffman, 2018).

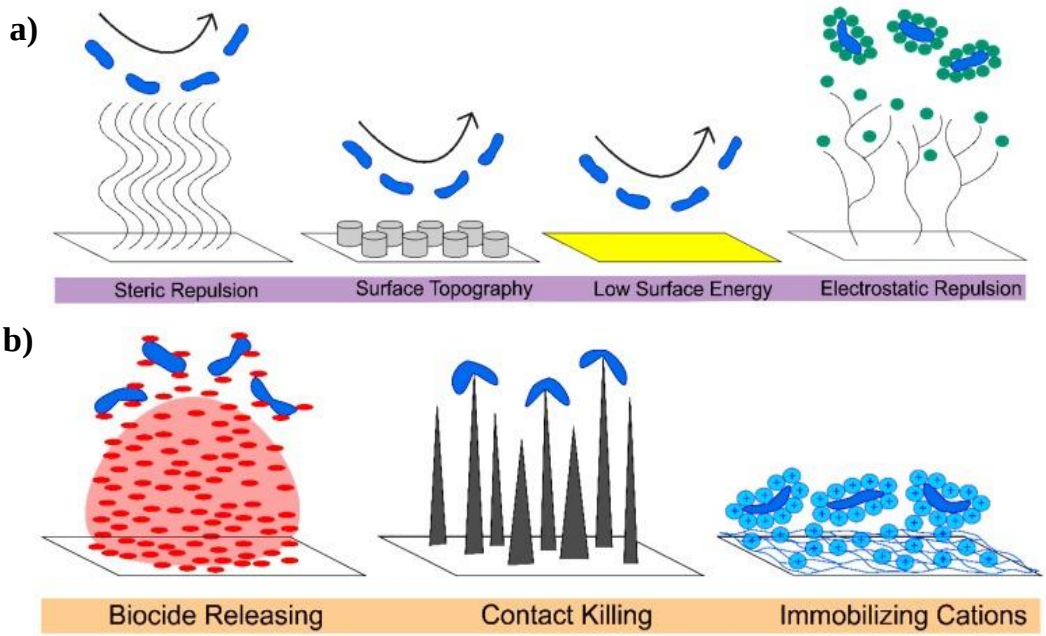

Figure 1.4 : Representation of antifouling surfaces **(a)** and antibacterial surfaces **(b)** (Kurtz & Schiffman, 2018)**.**

Releasing based antimicrobial surfaces can be performed using micro and nanotechnology to optimize the efficiency and suitability. Microneedle syringes and patches, nanoporous covers, polymeric patches, microparticles are examples of these technologies (Santos et al., 2014). Antibacterial agents are applied to the surfaces with physical adsorption, loading in the polymer matrix, complexation, or conjugation. The most important benefits of releasing antibiotics directly to the implant site are increasing its effectiveness and prevention of high dose usage. Releasing rate, dosage and controllability of antimicrobial agents affect the efficiency of the system. These factors can be adjusted by changing the properties of the antibacterial agent carrier such as type or degradability of polymer, and the size or shape of the drug carrier (Francolini et al., 2017).

1.4 Controlled Drug Delivery

Drug delivery system is a method used to transport drugs to desired tissues or organs safely with various carriers. The purpose of drug delivery systems is to improve the performance of drug therapy by reducing side effects, preventing drug aggregation, and increasing bioavailability. The delivery systems are able to design using different strategies like controlled-release strategy, targeted drug delivery strategy, or self-assembled drug delivery strategy (C. Li et al., 2019). Controlled release are systems where the drug is released to the patient at a predetermined rate and times. It provides a constant level of drug concentration in the blood plasma thus enhances therapeutic activity and reduces toxicity due to dose frequency (N. Sharma et al., 2015). The controlled released systems can be diffusion controlled, dissolution controlled, stimuli controlled or combination of them (Figure 1.5). In diffusion-controlled systems, when drug carriers contact the liquid solution, drug releases from higher concentration to lower concentration. Surface area and water absorbency of the carrier, and osmotic pressure of medium are factors that affecting the rate of release. (Son et al., 2017).

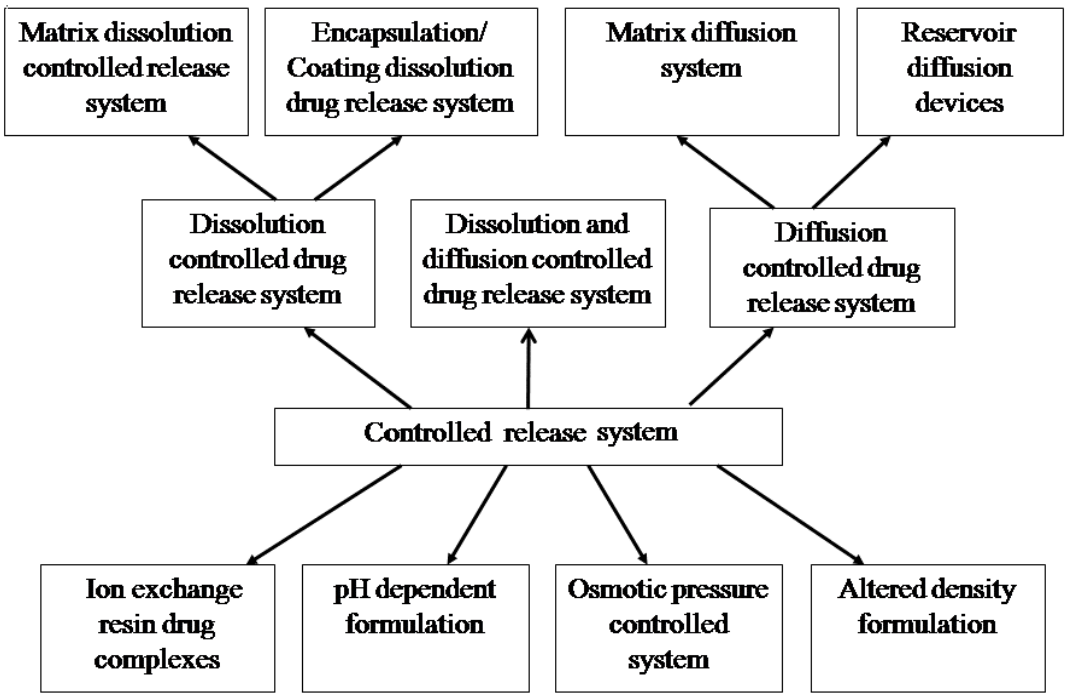

Figure 1.5 : Schematic representation of controlled release systems (A. Sharma et al., 2018).

Polymers used in drug delivery systems should be non-toxic, non-allergic, reproducible and if it is biodegradable polymer in vivo, structures formed after disintegration should be used in metabolism. Biodegradable polymers used in drug release system can be natural or synthetic. Synthetic polymers provide greater flexibility as they can be adjustable to individual needs, and natural polymers are cheap and can modify chemically (Santos et al., 2014).

1.4.1 Chitosan

Chitosan is a natural cationic polymer obtained by deacetylation of chitin which is a polysaccharide produced from the exoskeleton of shellfish such as shrimps, lobsters, crabs (Figure 1.6) and also from cell walls of fungi and insect. Chitosan composed glucosamine and N-acetyl glucosamine. At acidic pH, polymer becomes positively charged because of its amino groups, so it is insoluble at pH values above 7 (Campos et al., 2017). Chitosan is used in the pharmaceutical, cosmetic and food industry, agriculture, biotechnology and medical application. It is biocompatible, biodegradable, biorenewable, nontoxic, and easily used as films, membranes, sponges, and scaffolds, beads, microparticles, etc. Because of these features, chitosan is

generally preferred in biomedical applications such as tissue engineering, wound healing, gene delivery, and drug delivery (Elgadir et al., 2015; Jayakumar et al., 2010).

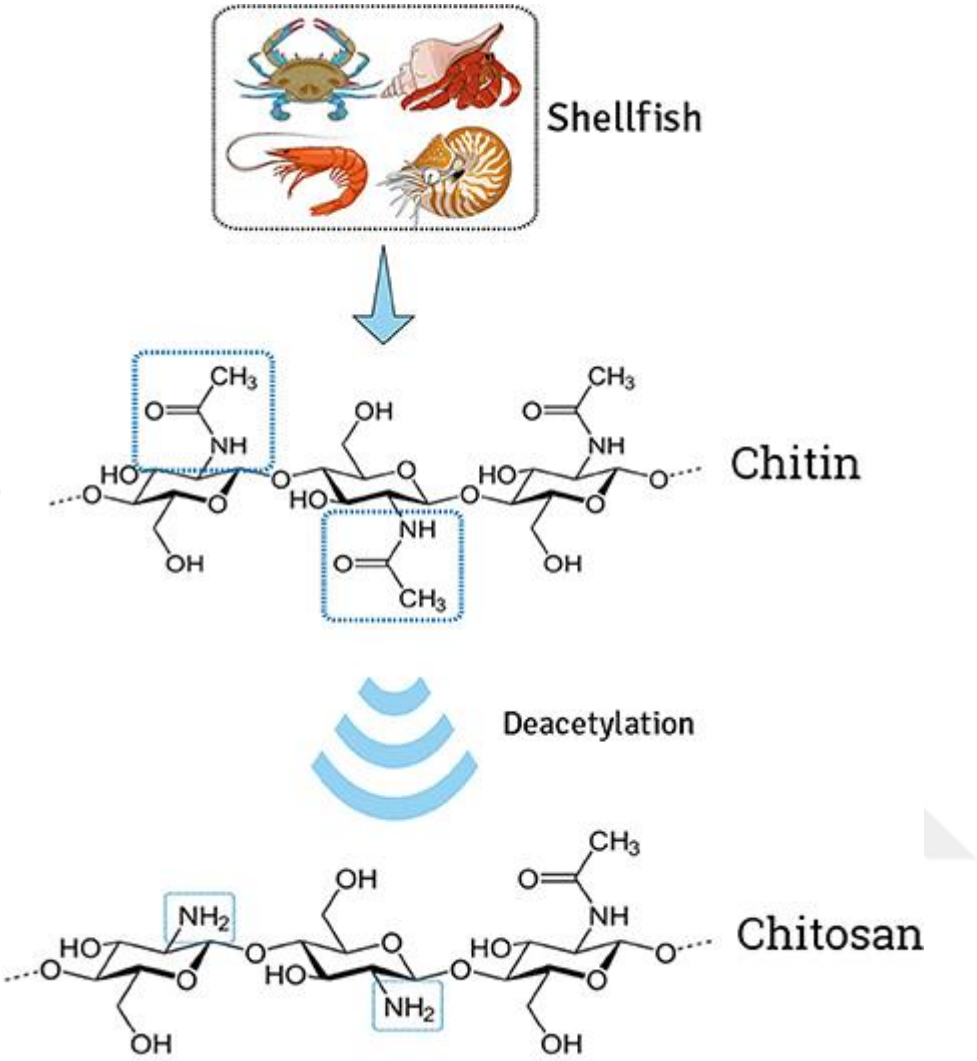

Figure 1.6 : Representation of obtaining chitosan (Campos et al., 2017).

Chitosan is the most preferable matrix molecule for drug delivery system because of two main features which are the molecular weight and degree of acetylation. Since these properties affect water solubility and hydrophobicity, they change drug encapsulation efficiency in drug delivery systems. Under acidic conditions, solubility of chitosan increases largely due to the protonation of the amino groups unlike under neutral and basic conditions, so it is used pH-sensitive application. In addition these major properties, chitosan is used as a drug carrier and coating molecule due to the presence of functional groups that facilitate chemical modifications and their biodegradable properties (Ahsan et al., 2018).

Glutaraldehyde is used for crosslinking of chitosan. Aldehyde groups of glutaraldehyde react with amino groups of chitosan (Kildeeva et al., 2009). Crosslinking process of chitosan with glutaraldehyde can be seen in Figure 1.7.

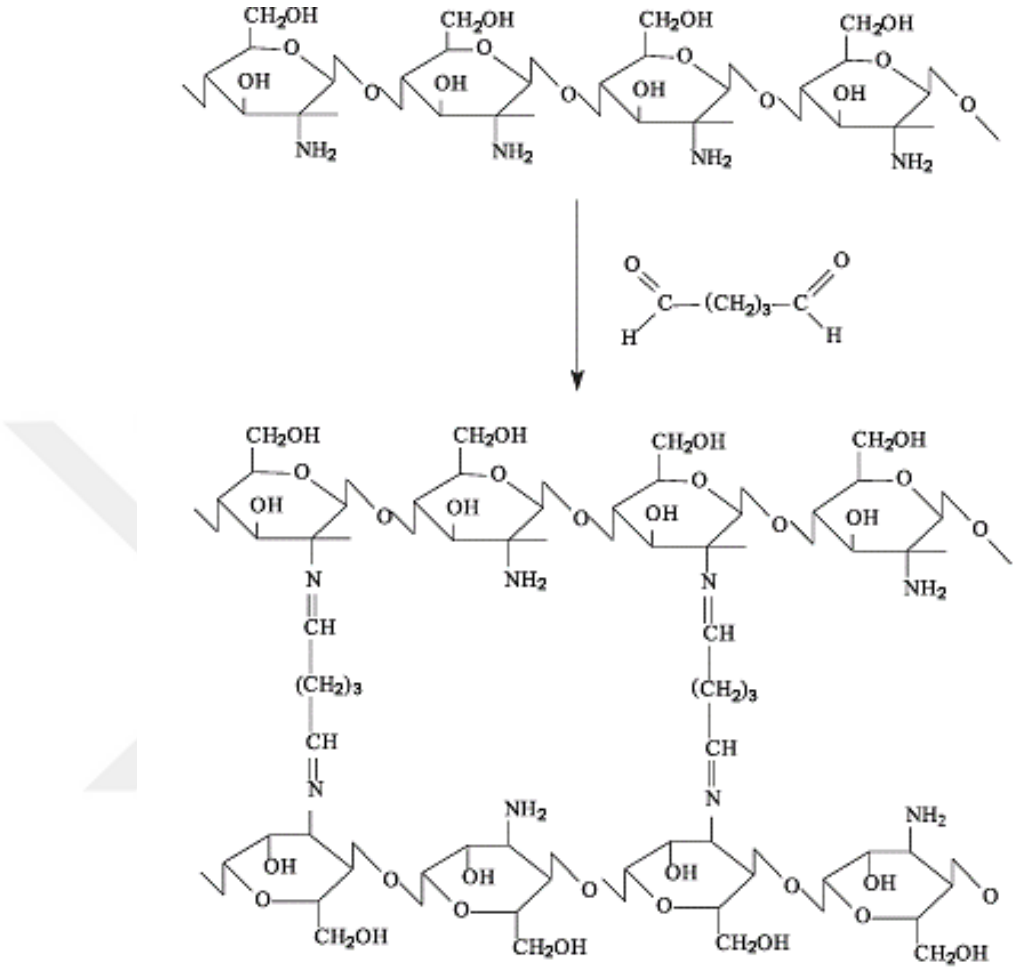

Figure 1.7 : Crosslinking process of chitosan with glutaraldehyde (Gonçalves et al., 2005).

1.4.2 Microspheres as drug carriers

Microspheres are solid powders, which can be prepared with natural and synthetic materials. Microsphere based drug delivery systems allow the drugs to be adapted to the specific application area through the combination of various polymers. These systems control the release of bioactive agents and provide effective dosage (N. Sharma et al., 2015). Microspheres can be produced by various techniques which are spray-drying, solvent evaporation, precipitation, emulsion crosslinking, ionotropic gelation, etc. In the emulsion crosslinking method, particles are prepared by emulsifying the polymer aqueous solution in the oil phase. A suitable surfactant is used

to stabilize the aqueous droplets and crosslinker is used to improve the mechanical properties of the particles. The size of the microspheres can be controlled by adjusting the stirring rate and amount of the crosslinker during the emulsion formation (Nair et al., 2009).

1.4.3 Ciprofloaxacin

Ciprofloxacin (Figure 1.8) is a second-generation fluoroquinolone and have antibacterial activity. Ciprofloxacin blocks bacterial DNA synthesis and it is very active against gram-positive and gram-negative organism. It is used as a medicine in the treatment of various human clinical infections, such as urinary tract infections, bone and soft tissue infections and respiratory tract infections (Adikwu & Brambaifa, 2012). The isoelectric constant (pI) of ciprofloxacin is 7.14 (P. C. Sharma et al., 2010) so it is negatively charged at above its pI value.

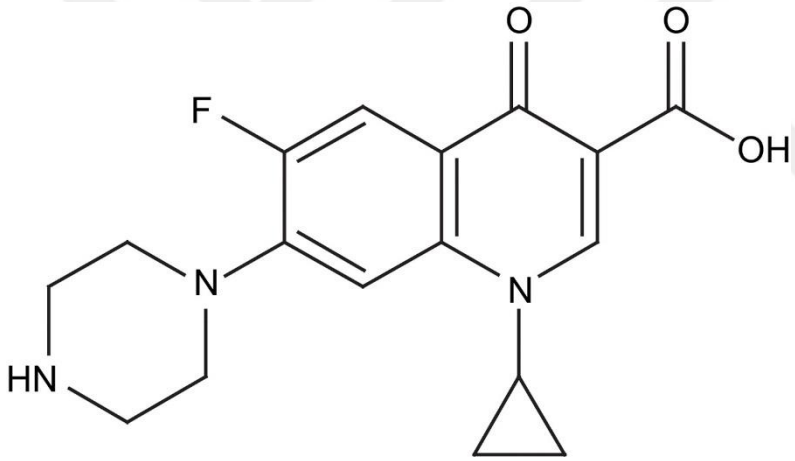

Figure 1.8 : Stucture of ciprofloxacin (P. C. Sharma et al., 2010).

2. MATERIALS AND METHODS

2.1 Materials

Chitosan from shrimp shells (product No: 50494), mineral oil (molecular biology reagent; product No: M5904), ciprofloxacin (product No: 17850), span 80 (product No: 85548), glutaraldehyde grade II (product No: G6257), 3-aminopropyltriethoxysilane (APTES), (98%, product No: A3648), toluene (product No: 108325), hexane (product No: 208752), sodium phosphate dibasic (Na_2HPO_4) (product No: 255793), calcium chloride dihydrate ($CaCl_2$) (product No: C1016), sodium chloride (NaCl) (product No: 134239), potassium phosphate monobasic (KH_2PO_4) (product No: P5379), potassium chloride (KCl) (product No: P9541), hydrofluoric acid (HF) (product No: 695068), nitric acid (HNO_3) (product No: 438073) and ethanol (C_2H_5OH) (96%, product No: 32205) were purchased from Sigma-Aldrich. Acetic acid (glacial) (product No: 901.013.2500) and sodium hydroxide (≥ 99 %, NaOH) (product No: 969.112.1000) were purchased from Isolab Chemicals. Titanium plate (grade 2) was purchased from Bag-San. Distilled water was used for the preparation of aqueous solutions.

2.2 Methods

2.2.1 Synthesis of the chitosan microspheres

Chitosan microspheres were prepared by using the water-in-oil (w/o) emulsion/cross-linking method. Briefly, 0.1 g chitosan was dissolved in 5 ml acetic acid (0.1 M). Then, mineral oil (50 ml) and Span 80 (1000 µl) were mixed with an overhead stirrer (500 rpm) for 10 minutes at room temperature. The polymer solution was added dropwise to the oil mixture and stirred. After 30 minutes, 400 µl of 25% glutaraldehyde (GA) was added dropwise to the oil-polymer solution for cross-linking and stirred for another hour. The mixture was incubated at 60°C for 1.5 hours and synthesized microspheres were washed three times with hexane. Microspheres were dried at 37°C for a day and were stored in the desiccator until use.

Drug loaded microspheres were prepared with same procedure by adding 1 ml ciprofloxacin (500 µg/ml) to chitosan – acetic acid solution (%2) (Figure 2.1).

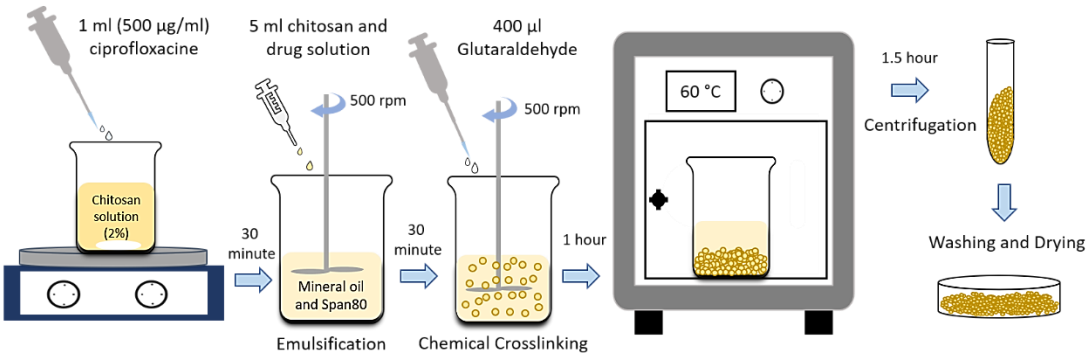

Figure 2.1 : Schematic representation of drug loaded microsphere synthesis.

2.2.2 Size analysis of microspheres

The diameter of the dried chitosan microspheres was analyzed with randomly selected hundred microspheres by using light microscope (Olympus BX60). The surface morphology of the microspheres was observed by a scanning electron microscopy (SEM, FEI Quanta- 600 FEG). For the SEM analysis, dried microspheres were fixed to carbon tape and coated with platinum.

2.2.3 Preparation and characterization of titanium surfaces

2.2.3.1 Surface modification of titanium plates

Titanium plates (1.5 × 1.5 cm^2) were polished with a mixture of 40 ml HF, 90 ml HNO_3 and 70 ml dH_2O. Polished samples were treated with sodium hydroxide (NaOH, 5M) solution for 24 h at 60˚C then samples were washed and dried at 60°C for 24 hours. Alkali treated surfaces were immersed in 5 % APTES solution and incubated at room temperature for 24 hours (Figure 2.2). Samples were washed sequentially with toluene, ethyl alcohol and distilled water. Washed samples were dried at 37°C and stored in the desiccator until use.

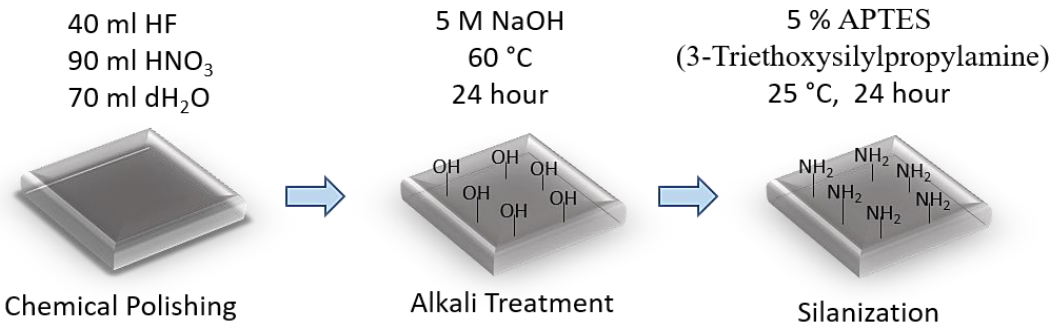

Figure 2.2 : Schematic representation of surface modification of titanium plates.

2.2.3.2 Immobilization of microspheres

Microspheres were entrapped on the surface of titanium plates with chitosan film (Figure 2.3). For the immobilization, homogeneous mixture of chitosan (2% w/v) and microspheres was prepared. This mixture was spread as thin layer on titanium surface activated with GA (8%) for 1 hour. Coated surfaces were kept at room temperature for 30 minutes and frozen at -20 ° C (30 min) before lyophilization. Different chitosan to microsphere ratios (100:5, 50:10 and 50:5 (µl: mg)) were used for the immobilization to obtain high microsphere loading without any stability problem.

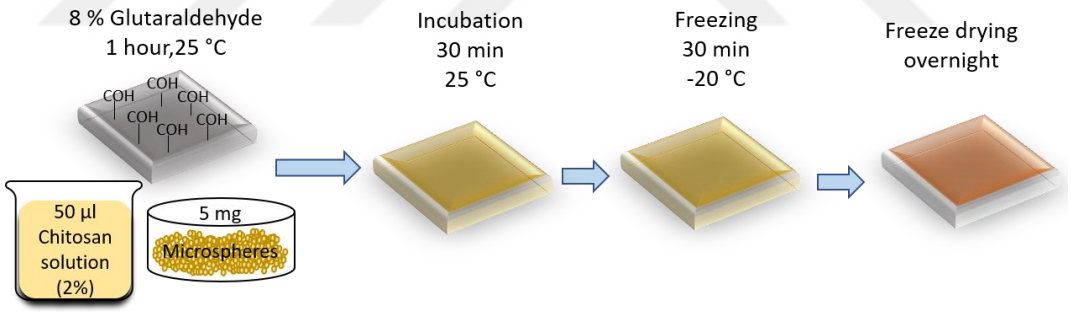

Figure 2.3 : Schematic representation of microsphere immobilization on titanium plate**s.**

2.2.3.3 Nano hydroxyapatite (nHA) coating

For the nano hydroxyapatite formation, procedure based on electrostatic interaction with free -OH groups and coordinated binding with $-NH_2$ groups on the chitosan surface at high pH was followed (M. Li et al., 2013). $CaCl_2$ solution (1.25 mM, 20 ml) was prepared and pH of the solution was adjusted to 10 using NaOH (2 M). Samples were immersed in prepared solution at 37 ° C and were stirred for an hour. Then, 20 ml Na_2HPO_4 solution (0.75 mM) was prepared and its pH was adjusted to 10. Prepared solution was added dropwise in the mixture and the pH of the medium was adjusted to

10 again. After 1 hour, samples were taken from the shaker and incubated at 37°C for 24 hours. Samples washed with dH_2O and dried at 37 ° C (Figure 2.4). In addition, chitosan sponges were prepared to observe nHA deposition on chitosan. For this, prepared chitosan solution (%2) was frozen at 24-well plates (1 ml/well) and freeze-dried for a day. HA coating process was carried out not only on microspheres immobilized Ti surfaces but also for chitosan sponges and free microspheres as control.

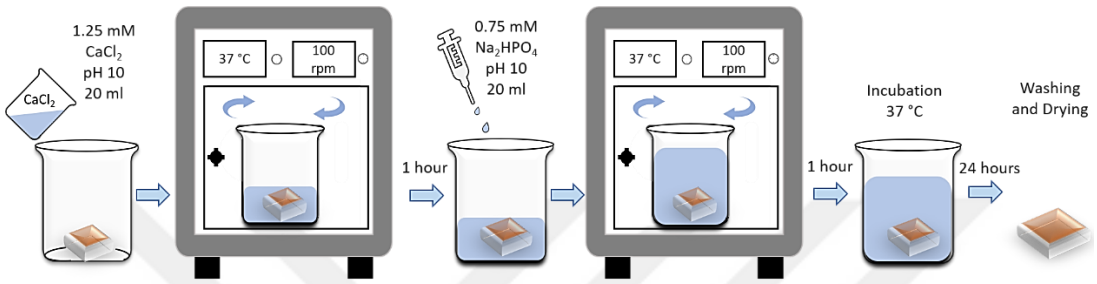

Figure 2.4 : Schematic representation of nano hydroxyapatite coating.

2.2.3.4 Characterization of titanium surfaces

The chemical composition of activated titanium surfaces and the crystal structure of nHA was analyzed with Fourier transform infrared spectroscopy (Perkin-Elmer Spectrum One FT-IR) and X-ray diffraction spectroscopy (XRD, Philips PW3710). The presence of calcium and phosphorus on the surfaces were analyzed with energy-dispersive X-ray spectroscopy (EDS, JEOL JSM 7000F). The morphology of the activated titanium surfaces and microsphere immobilized surfaces was observed by scanning electron microscopy (SEM, FEI Quanta- 600 FEG).

2.2.4 Drug release studies

The release profiles were studied in phosphate-buffered saline (PBS) at pH 7.4. Drug loaded samples were immersed in 3 ml PBS and were placed on orbital shaker (100 rpm) at 37 ° C. Release medium (3 ml) was removed periodically for analysis and fresh PBS of the same volume was added. The removed PBS was analyzed with a spectrophotometer at 278 nm and the amount of released ciprofloxacin was calculated by using the calibration curve. Drug release studies were carried out for free microspheres and immobilized microspheres (HA-coated and uncoated).

3. RESULTS AND DISCUSSION

3.1 Sizes of Chitosan Microspheres

The effect of the stirring rate on chitosan microspheres was analyzed using three different stirring rates (300, 400 and 500 rpm). Microspheres were analyzed under light microscope and seen that microsphere size was inversely related to stirring rate as expected (Figure 3.1).

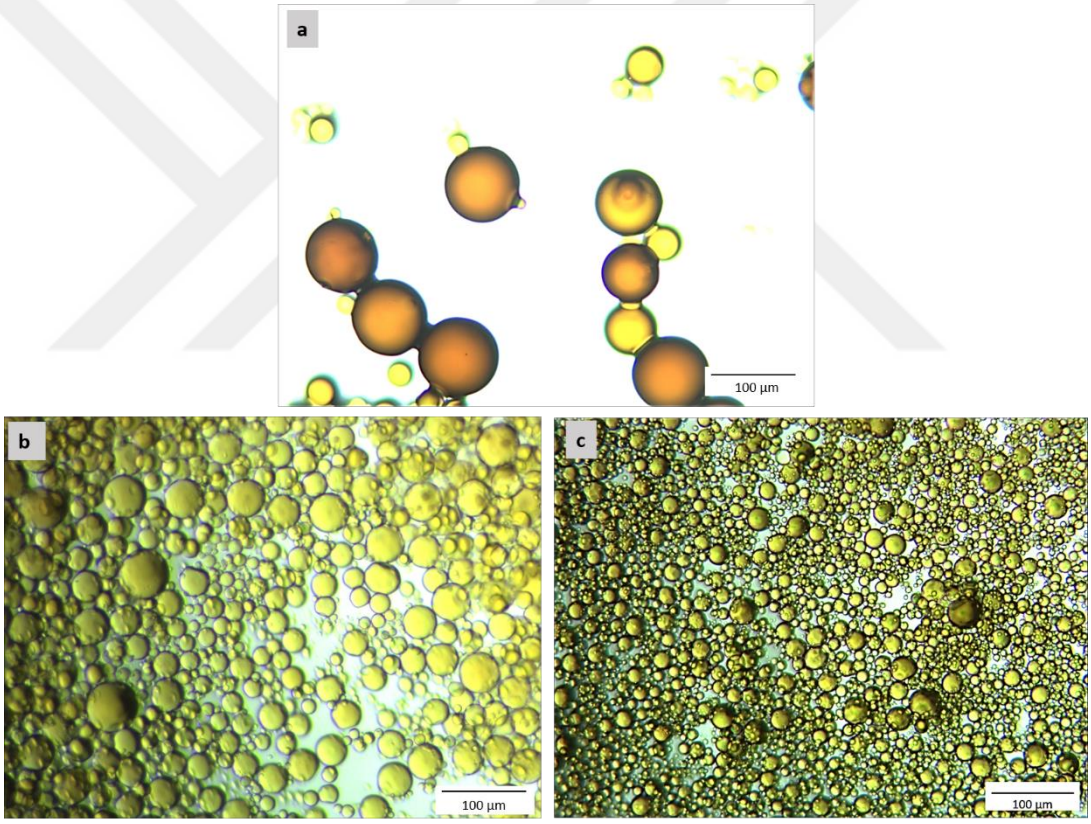

Figure 3.1 : Light microscope images (10x) of microspheres prepared at **a)** 300 rpm **b)** 400 rpm and **c)** 500 rpm stirring rate.

The size of the microspheres was measured by using hundred randomly selected microspheres. The average diameter of microspheres was calculated as 61.0 ± 20.6 µm at 300 rpm, 48.8± 11.4 µm at 400 rpm and 19.2 ± 6.5 µm at 500 rpm. The distribution plot and microscope analysis showed that when the stirring rate was ncreased, the size distribution of the microspheres became narrower and more homogenous (Figure 3.2).

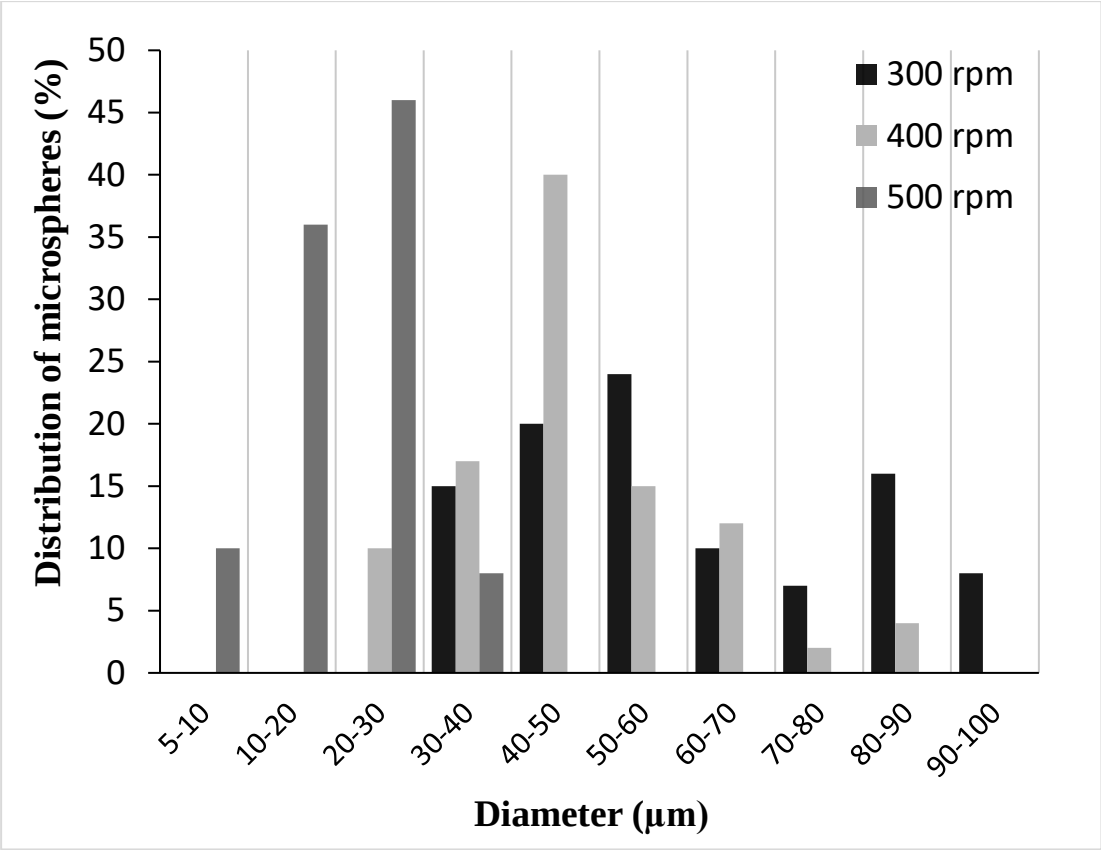

Figure 3.2 : Size distribution of the microspheres prepared at different stirring rates.

According to these results, microspheres prepared at 500 rpm are more homogenous and since they have smaller diameter, their surface area to volume ratio is higher. This value was therefore selected for the immobilization in future studies.

In addition, SEM was used to examine the microsphere morphology. Analysis of microspheres prepared at 500 rpm showed smooth and spherical appearance (Figure 3.3).

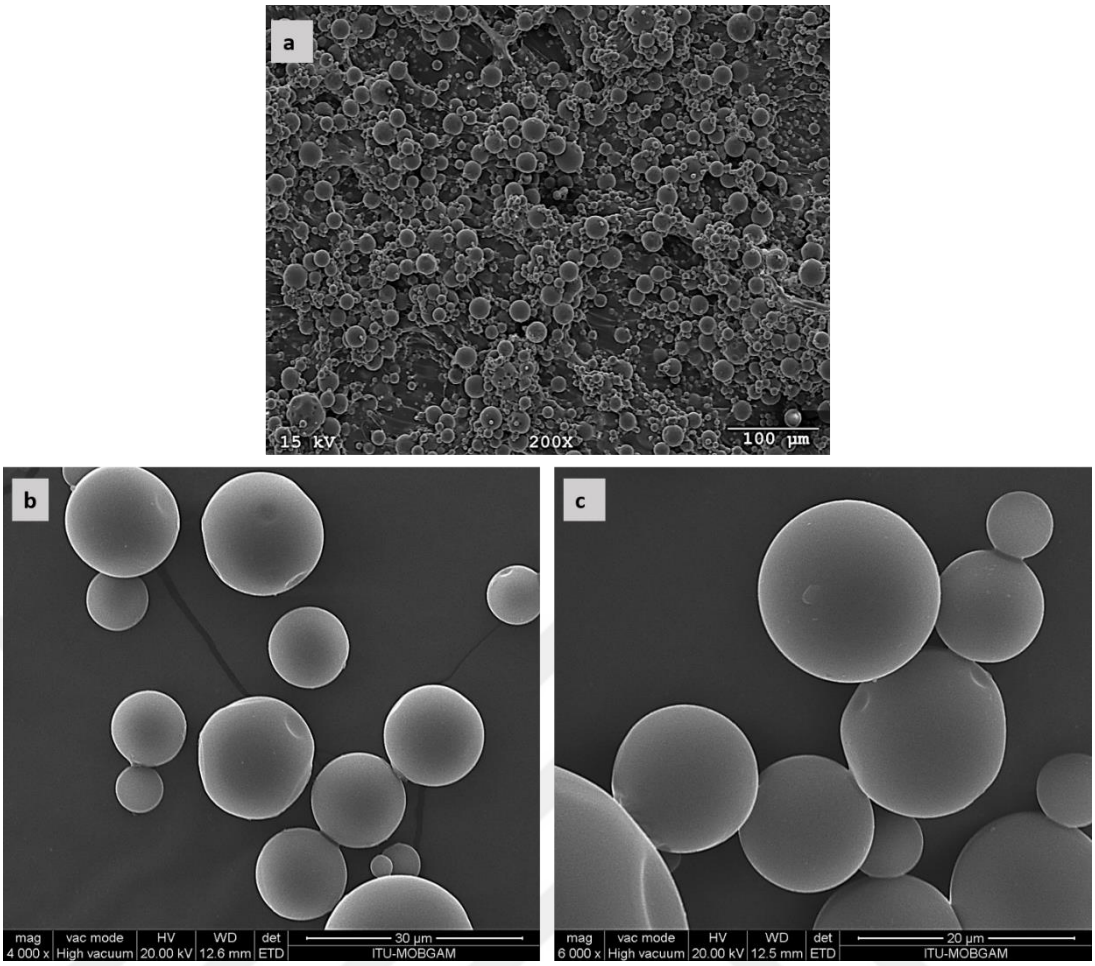

Figure 3.3 : SEM micrographs of microspheres prepared at 500 rpm at **a)** 200x and **b)** 4000x **c)** 6000x magnifications.

3.2 Characterization of Surface Modified Titanium Plates

SEM was used to examine the morphology of the activated Ti surfaces. Figure 3.4 shows that after the alkali treatment, porous structures were formed on Ti surfaces. The porous structure changed after the silanization but still preserved. As a result, morphological changes which may improve biocompatibility were observed since the roughness increases available surface for cell attachment (Cuellar-Flores et al., 2016).

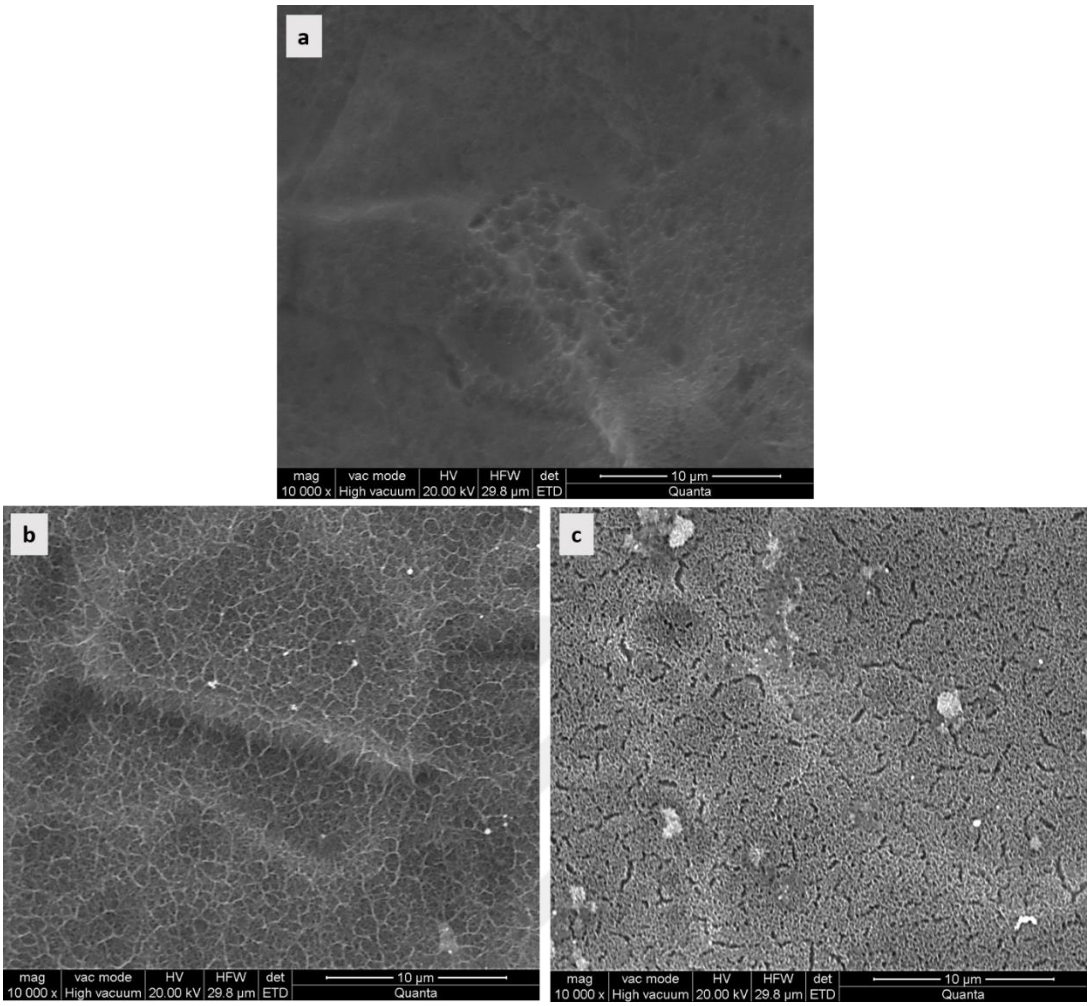

Figure 3.4 : SEM micrographs of Ti surfaces (10.000x) **a)** polished **b)** alkali treated **c)** silanized.

FTIR analysis was carried out for alkali treated and silanized surfaces to determine the chemical groups on the surfaces and, characteristic peaks were shown in Figure 3.5. The presence of the hydroxyl group on alkali treated surface was detected. Peaks seen at 3684-2679 cm^{-1} indicates O-H stretching vibration and at 1638 cm^{-1} indicates O-H bending vibration (Kharbanda et al., 2017). The shoulder at 831 cm^{-1} indicate Na - O bending and broad peak at 633 cm^{-1} indicate Ti-O groups (Tsiourvas et al., 2011). According to FTIR analysis of silanized surfaces, characteristic peaks of APTES were detected at 1034 cm^{-1} due to the vibration of Si-O-Si bond and at 1121 cm^{-1} due to the vibration of the Si-OH group. Also, peaks at 1576 cm^{-1} and 1630 cm^{-1} are N-H vibrations of the pyramid amine and belong to the -NH2 groups that will be used for cross-linking with GA. The peak at 2933 cm^{-1} originates from the methylene group (-CH_2) and showed that the silane agent is bound to the surface (Kharbanda et al., 2017;

D. Li et al., 2013). These results indicate that -NH_2 groups are formed on the surface and the Ti plates are prepared for the cross-linking.

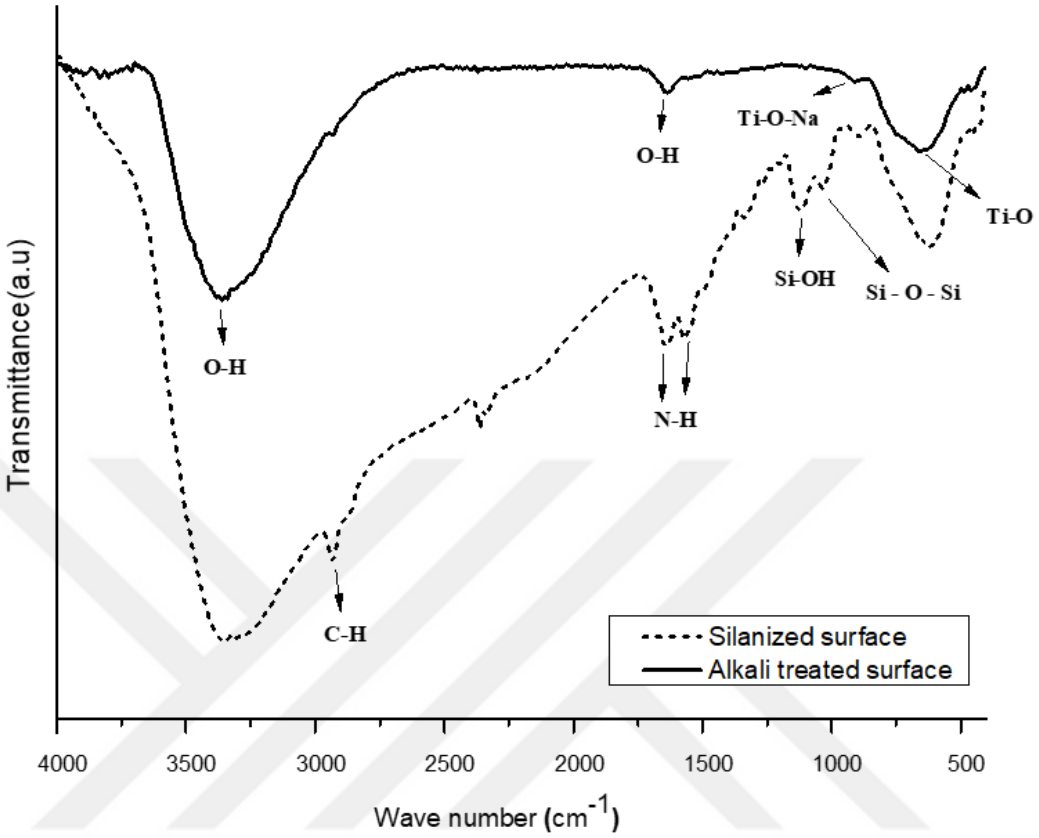

Figure 3.5 : FT-IR spectra of alkali treated and silanized Ti surfaces.

3.3 Optimization of Microsphere Immobilization

The amount of microsphere and chitosan solution required for immobilization was optimized. For this purpose, first the surfaces were coated with 100 µl chitosan solution (2%) and 5 mg microsphere (100:5, µl:mg). When prepared samples were analyzed with SEM, dense and non-uniform chitosan film was observed with small fractures and the microspheres were not evenly distributed (Figure 3.6). In addition, it was observed that when Ti samples were immersed in PBS, some areas swelled more and separated from the surfaces showing that non-homogeneous chitosan film may cause rapid disintegration from the surface.

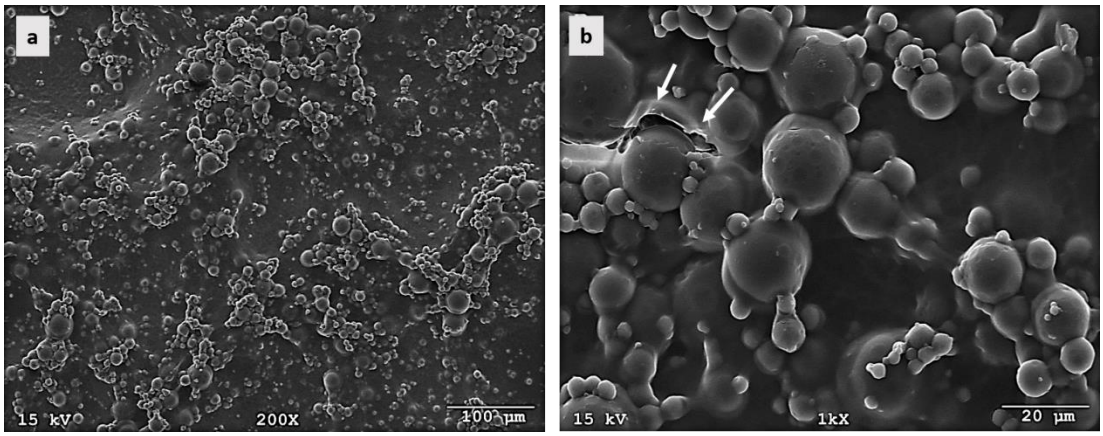

Figure 3.6 : SEM micrograph of the Ti surface coated with mixture of 100 µl chitosan solution and 5 mg microsphere (100:5, µl:mg) **a)** 200x and **b)** 1000x magnifications.

The amount of chitosan was therefore decreased, and the amount of microsphere was increased to obtain homogeneously dispersed chitosan film. For this purpose, surfaces were modified using a mixture of 50 µl chitosan solution and 10 mg microsphere (50:10, µl:mg). After the drying, regional fractures and flaking were observed in the SEM analysis (Figure 3.7). This showed that the quantity of microspheres is too much for the surface area and therefore, reduced.

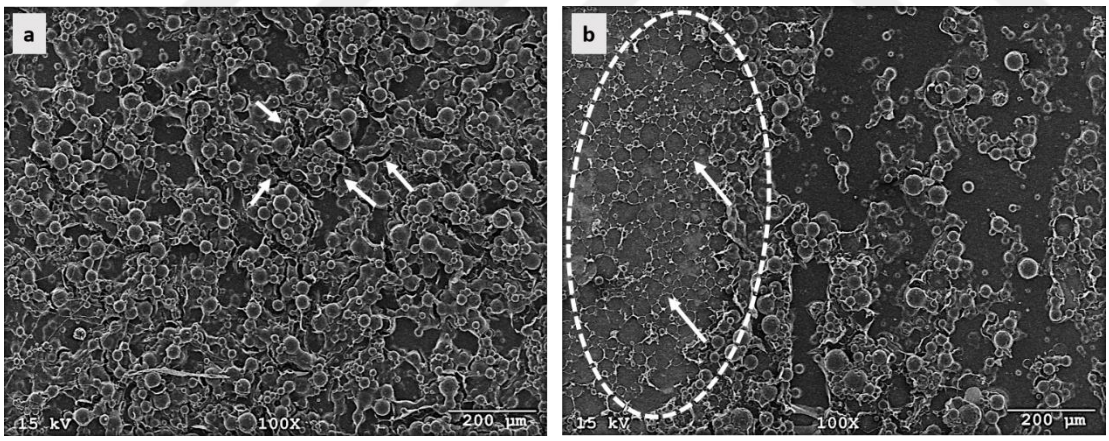

Figure 3.7 : SEM micrograph of the Ti surface coated with mixture of 50 µl chitosan solution and 10 mg microsphere (50:10, µl:mg). **a)** fractures of chitosan film (100x) and **b)** flaking of microspheres (100x).

Finally, 50 µl chitosan solution and 5 mg microsphere mixture (50:5, µl:mg) were applied to surfaces. After freeze-drying, fractures were not observed on the surfaces. When SEM analyses were done, it was observed that homogeneous coverage of the surface was achieved throughout the surface (Figure 3.8). Also, any flaking or separation was not observed on the Ti surfaces immersed in the PBS (30 days, 37 °C).

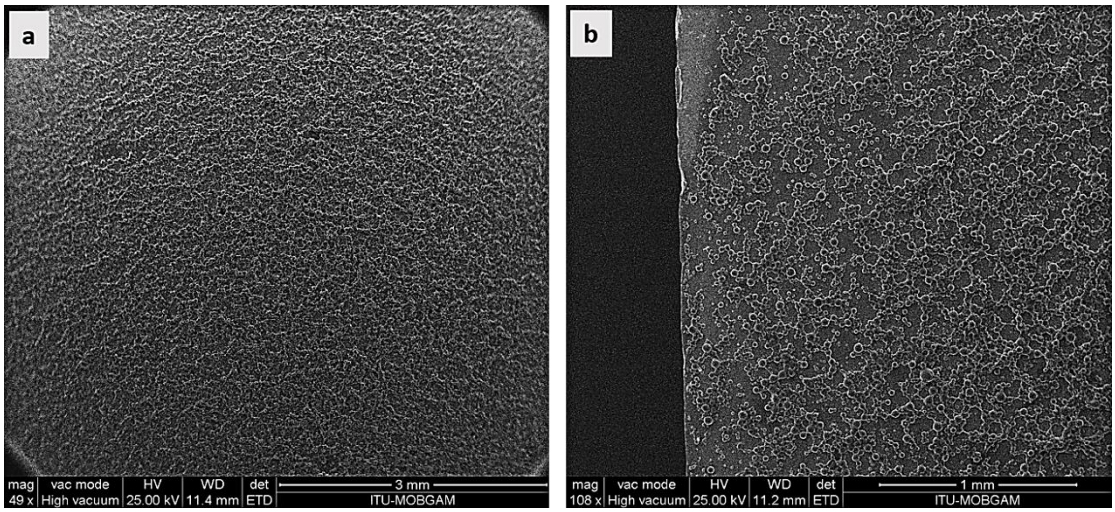

Figure 3.8 : SEM micrograph of the surface coated with mixture of 50 µl chitosan solution and 5 mg microsphere (50:5, µl:mg). **a)** 49x and **b)** 108x magnifications.

Different samples were prepared using the optimized amounts and were analyzed to determine the reproducibility. It was seen that homogeneous and stable coatings can be obtained reproducibly by this method (Figure 3.9).

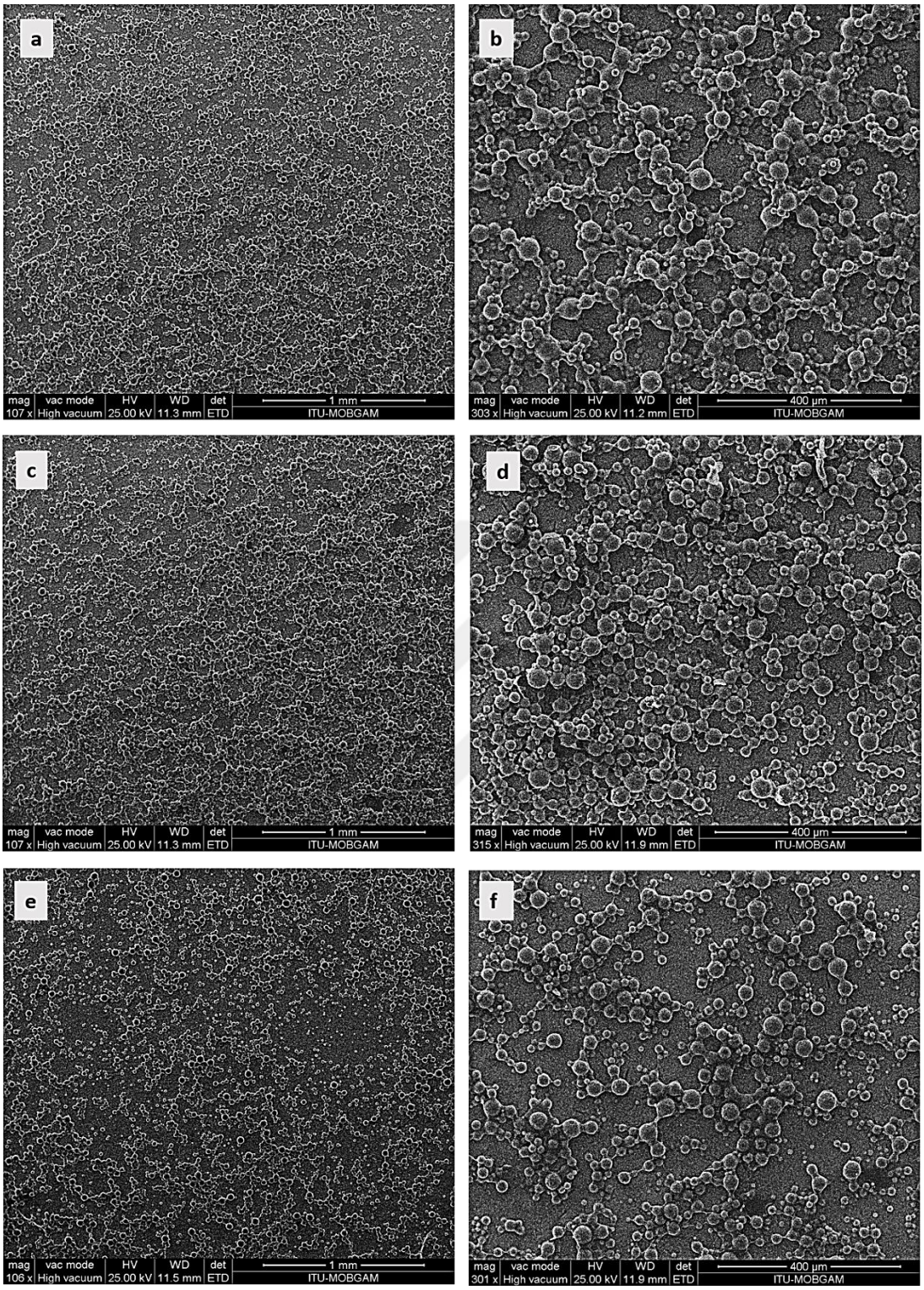

Figure 3.9 : SEM micrographs of 3 different samples (prepared with ratio of 50:5 (µl:mg)) **(a,b) (c,d)** and **(e,f)** at different magnifications:100x **(a,c,e)** and 300x **(b, d, f)**.

As a result, 1.5 cm^2 titanium surfaces were homogeneously coated using 50 µl chitosan solution and 5 mg microsphere. These optimized parameters were used for furthere studies.

3.4 Effects of Immobilization on Drug Release

Drug release studies were carried out with free and immobilized microspheres to examine the effect of immobilization on the release profile. It was seen that the drug released from free microspheres stopped at the end of 19 days (Figure 3.10). Therefore, releasable drug amount was determined to be 10.5 µg. This value was accepted as the total drug amount and percentage drug release was calculated.

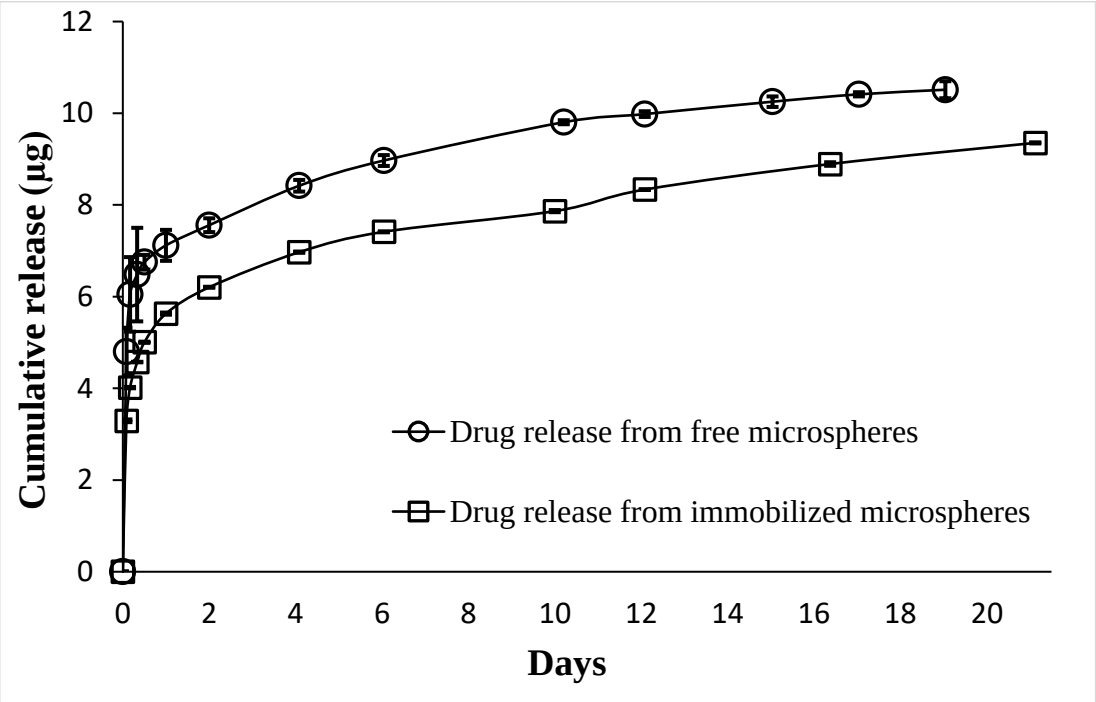

Figure 3.10 : Overall cumulative release of ciprofloxacin from free and immobilized microspheres.

Percentage release profile (24 h) was examined to analyze the burst release and it was observed that 67.7 % of the total drugs were released from the free microspheres after 24 h whereas this value is 53.6 % for immobilized microspheres (Figure 3.11). The decrease in burst release rate at immobilized microspheres was observed. The chitosan film which covered the microspheres on the Ti surface probably caused a slowdown in the drug release rate because of its thickness (Gulati et al., 2012).

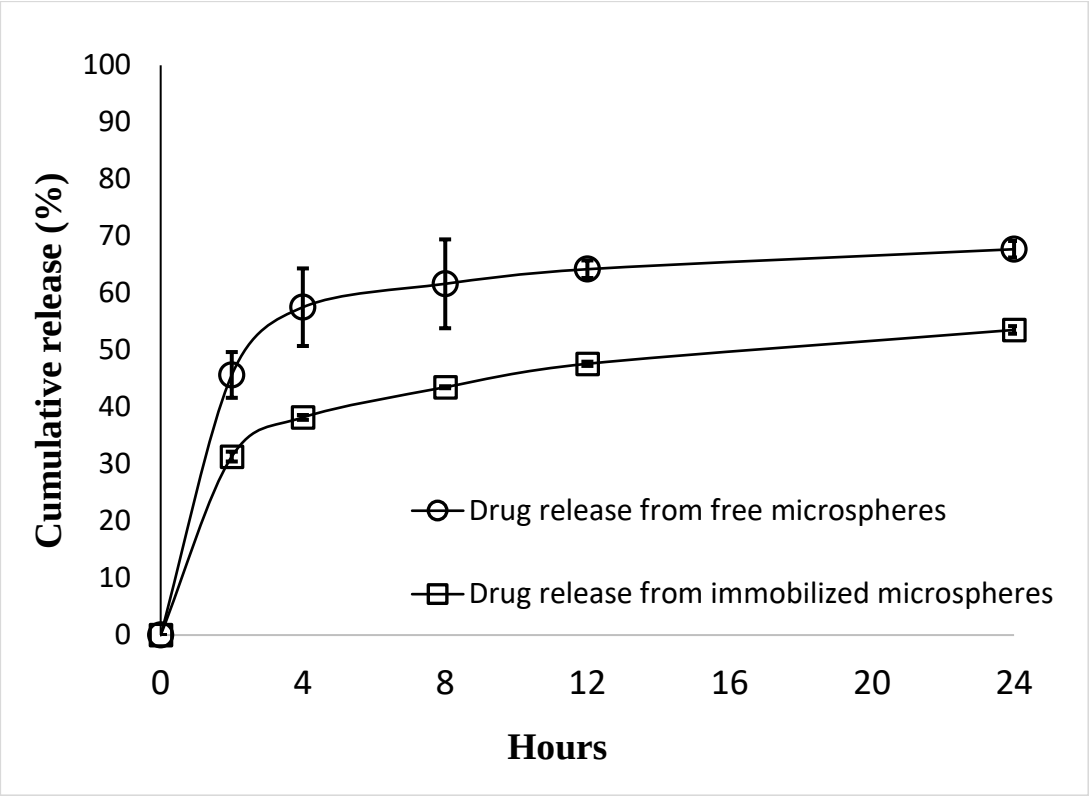

Figure 3.11 : Percentage cumulative release of ciprofloxacin from free and immobilized microspheres for 24 h.

3.5 Characterization of Nano Hydroxyapatite Coatings

3.5.1 FTIR analysis

Nano hydroxyapatite coatings were analyzed with FTIR. Two different peaks were detected at 563 cm^{-1} and 602 cm^{-1} indicating PO_4^{-3} group after the nano hydroxyapatite synthesis (Figure 3.12). Due to the characteristic peak of chitosan, the peak belonging to PO_4^{-3} group, which is expected to be seen at around 1040 cm^{-1}, was not observed. However, chitosan peak appeared to be sharper after the coating. These peaks matched the hydroxyapatite peaks, and this showed the presence of nHA on the microsphere surfaces (Zhe et al., 2011).

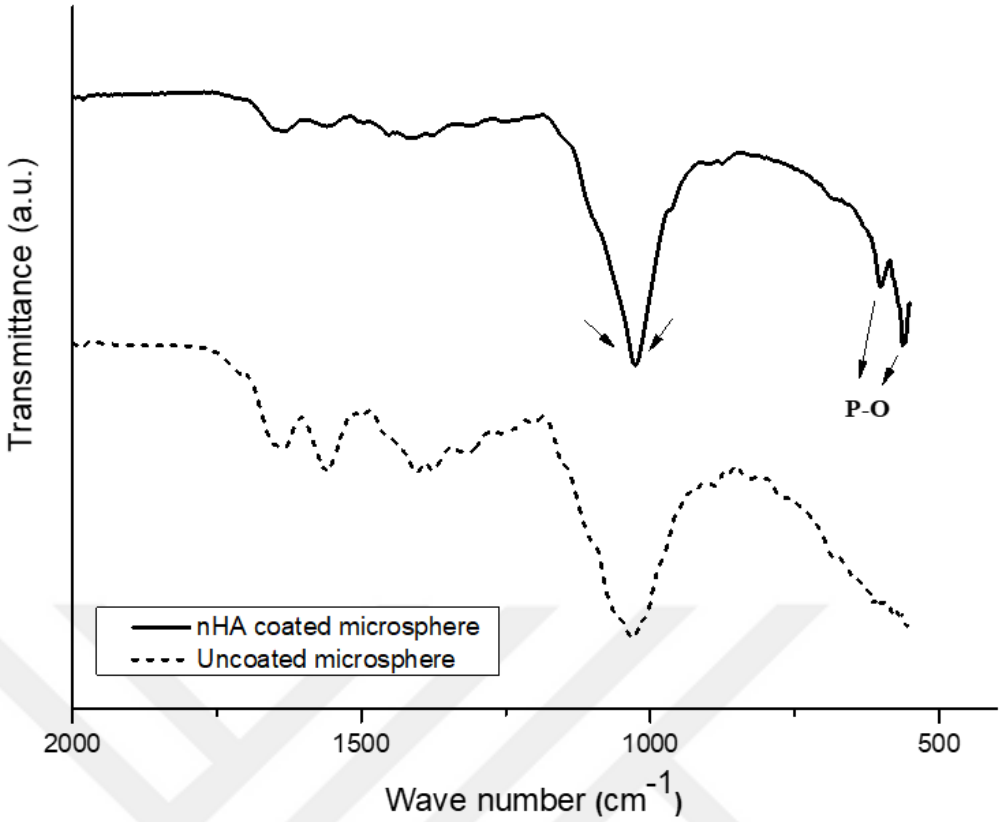

Figure 3.12 : FT-IR spectra of uncoated and nHA coated microspheres.

3.5.2 SEM and EDS analysis

Afterwards, the nHA coated microspheres were examined with SEM and EDS. Coatings can be clearly observed on microsphere surfaces as shown in Figure 3.13.

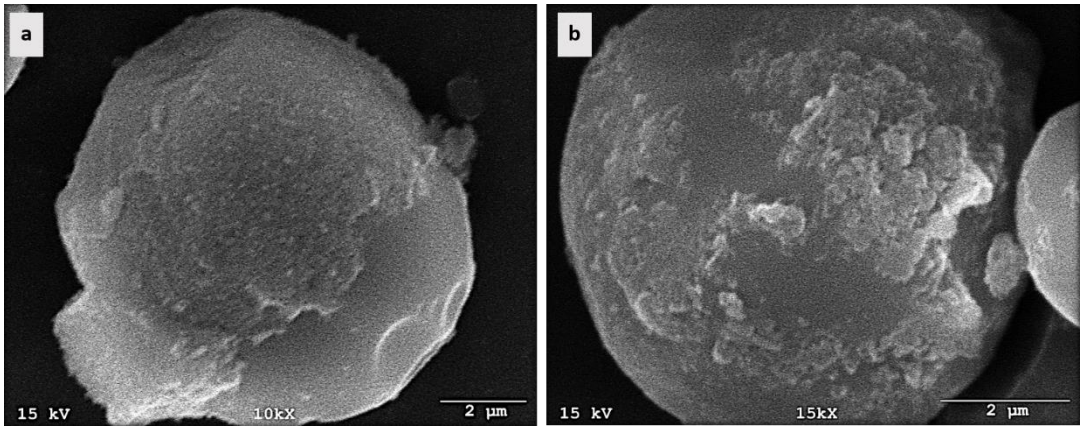

Figure 3.13 : SEM micrographs of nHA coated microspheres **a)**10.000x and **b)**15.000x.

EDS analyses of surfaces were also performed, and the presence of calcium and phosphorus was determined (Figure 3.14). Point analyses taken from different parts of

the microsphere showed that C/P ratio is different at different locations. Also, although nHA deposition can not be observed in the image in the region #1, the presence of calcium and phosphorus was detected by EDS. Therefore, it can be said that while thin nHA deposition was observed in this region, a thicker nHA deposition was observed in other regions (#2 and #3) where the amount of calcium and phosphorus is higher.

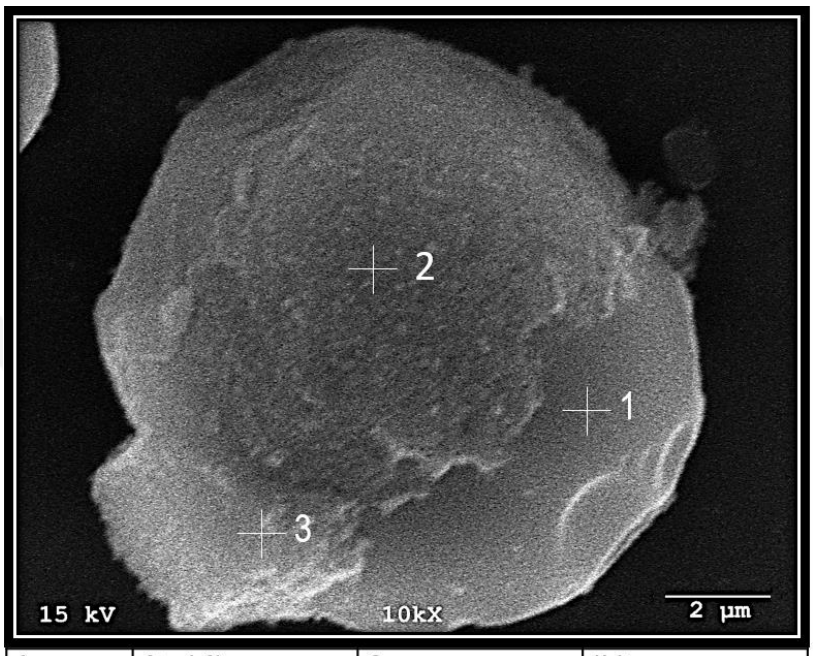

1	Atomic %	Conc	Units
P	30.393	26.765	wt.%
Ca	23.361	26.620	wt.%
2	**Atomic %**	**Conc**	**Units**
P	35.263	30.770	wt.%
Ca	35.084	39.613	wt.%
3	**Atomic %**	**Conc**	**Units**
P	38.433	32.851	wt.%
Ca	54.169	59.911	wt.%

Figure 3.14 : EDS analysis of nHA coated microsphere (10.000x).

Then, nHA deposition for chitosan sponge was determined since microsphere was immobilized with chitosan film. In SEM analysis, dense nHA deposition was observed on the chitosan sponges (Figure 3.15).

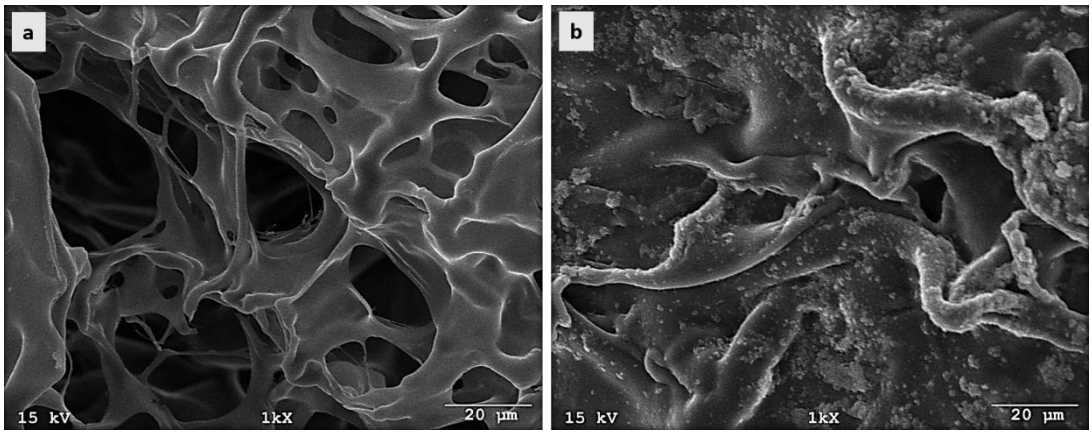

Figure 3.15 : SEM micrographs of chitosan sponges **a)** uncoated **b)** nHA coated (1000x).

Calcium and phosphorus amount for chitosan sponges were determined by EDS analysis (Figure 3.16). Similar to EDS results of nHA coated microsphere, it was observed that the amount of calcium and phosphorus was lower in some areas and higher in others.

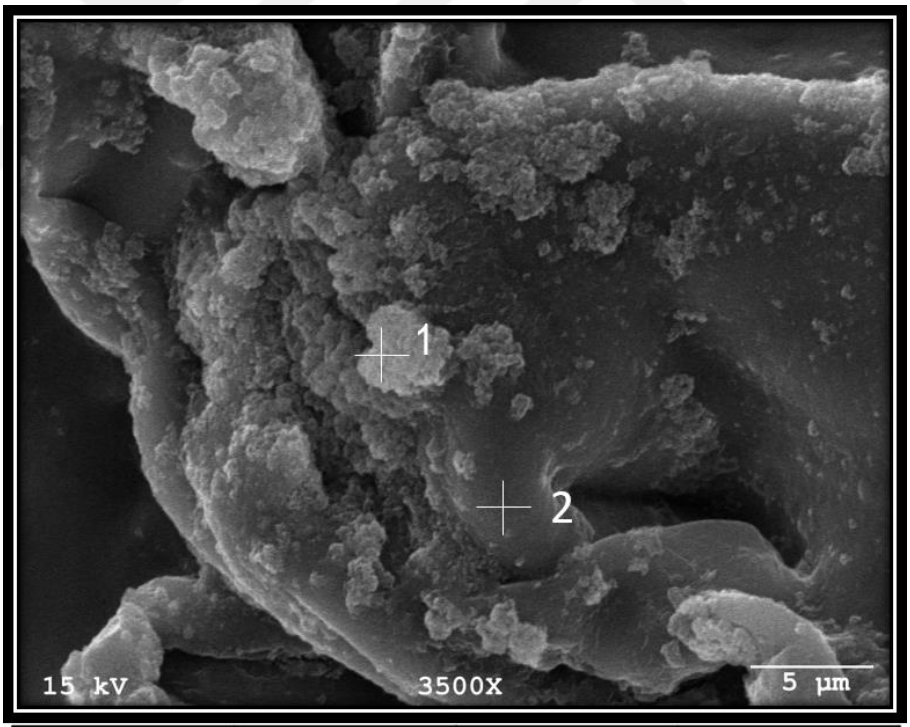

1	Atomic %	Conc	Units
P	20.730	23.678	wt.%
Ca	30.748	45.446	wt.%
2.	Atomic %	Conc	Units
P	10.690	14.939	wt.%
Ca	9.485	17.152	wt.%

Figure 3.16 : EDS analysis of nHA coated chitosan sponge (3500x).

Lastly, nHA deposition was investigated on the microsphere immobilized surfaces and characterization studies were performed. nHA deposition was observed on microsphere surfaces and chitosan coated areas (Figure 3.17). Arrows show the chitosan film, where there is no microsphere, was covered with nano hydroxyapatite (Figure 3.17 b).

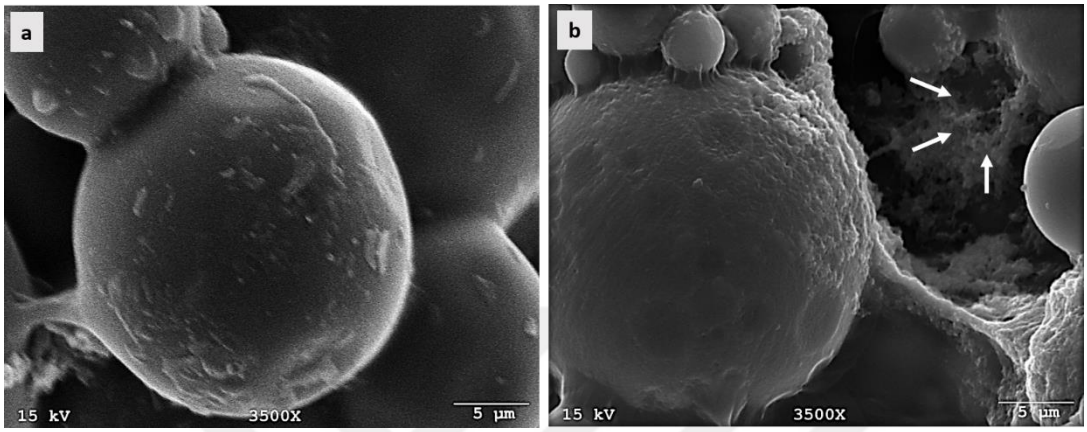

Figure 3.17 : SEM micrographs of nHA coated microsphere-chitosan modified Ti surfaces (3500x).

EDS analyses were also carried out for titanium surfaces to determine the amounts of calcium and phosphorus (Figure 3.18). Deposition was observed by EDS even in some areas where the image does not show any deposition (# 2). According to all EDS results, it was concluded that Ca and P deposition was seen on all surfaces, but it was not homogeneous.

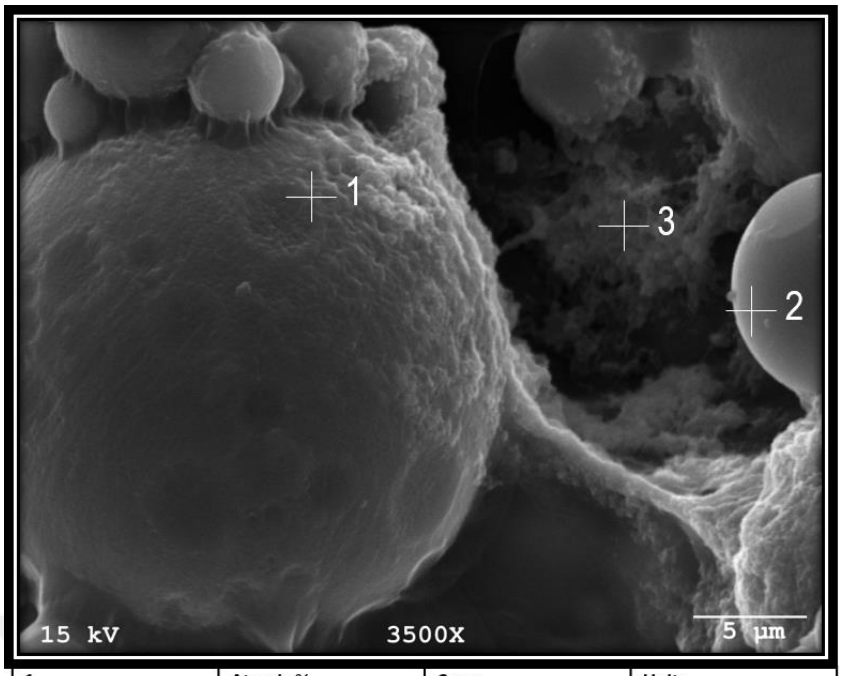

1	Atomic %	Conc	Units
P	6.353	12.316	wt.%
Ca	5.198	13.041	wt.%
2	Atomic %	Conc	Units
P	3.358	7.174	wt.%
Ca	1.188	3.283	wt.%
3	Atomic %	Conc	Units
P	14.943	21.587	wt.%
Ca	19.325	36.124	wt.%

Figure 3.18 : EDS analysis of nHA coated Ti surface.

3.5.3 XRD analysis

Finally, nHA coated chitosan-microsphere modified Ti surfaces were characterized with XRD to identify the crystal structure. It can be seen that although peaks around 2Θ = 31°, 32°, 39°, and 45° were observed (Figure 3.19 b) as characteristic peak of HA, some of them were not observed (Salah et al., 2014). This may be demonstrated that poorly crystalline (Reyes-Gasga et al., 2013) or thin layered nHA formed on the Ti surface.

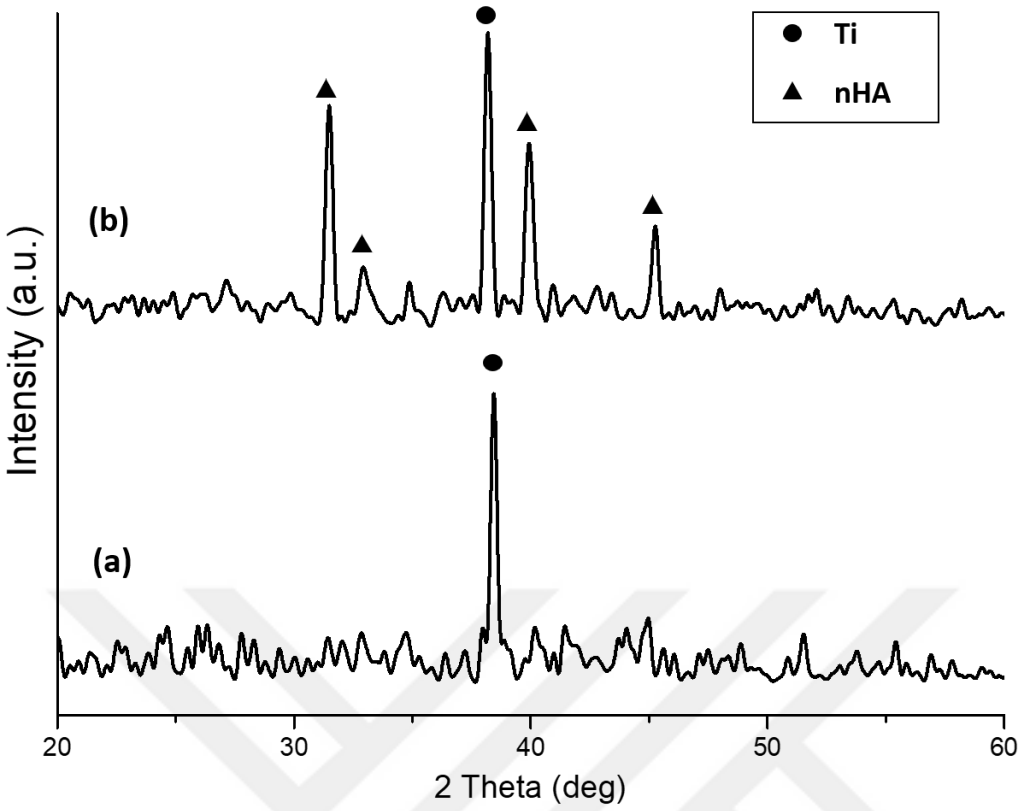

Figure 3.19 : XRD patterns of **a)** uncoated **b)** nHA coated chitosan-microsphere modified Ti surfaces.

3.6 Stability of Whole System

After all analysis, the stability of nHA coated microsphere-chitosan modified Ti surfaces was studied. For this purpose, surfaces were immersed in PBS (0.01 M, pH 7.4) for 30 days. SEM analysis was showed that even after 30 days no any fracture or flaking on surfaces were seen (Figure 3.20).

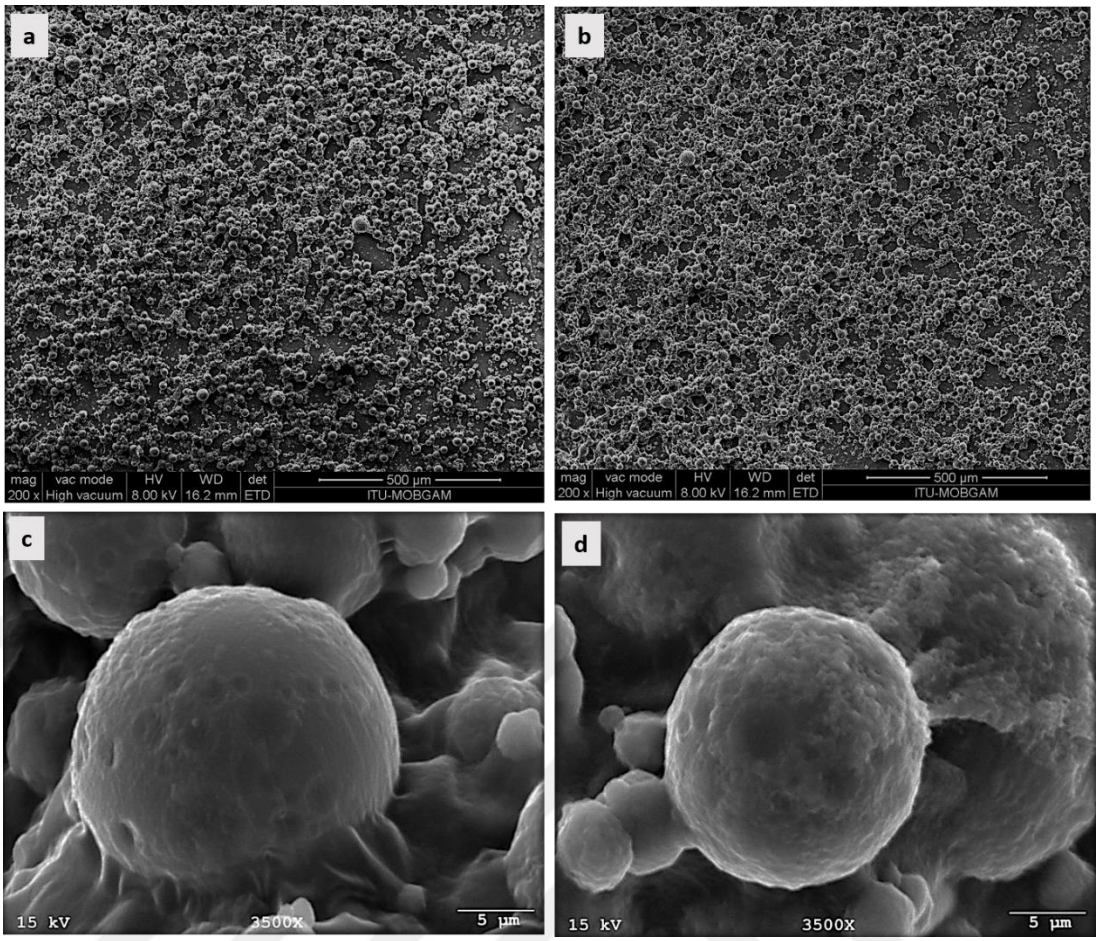

Figure 3.20 : SEM micrographs of nHA coated microsphere-chitosan modified Ti surfaces after keeping in PBS (30 days).

As a result, microspheres were successfully immobilized on titanium surfaces and were coated with nHA.

3.7 Effects of Nano Hydroxyapatite Coatings on Drug Release

Drug release studies were also performed for nHA coated microsphere-chitosan modified Ti surfaces to examine the effects of nHA coatings on release profile. As can be seen in Figure 3.21, uncoated microspheres released 9.35 µg drug in 21 days, while the nHA coated microspheres released 8.46 µg drug. A decrease in the amount of released drug was observed after the nHA deposition. This decrease may be originated from the drug loss occurred during nHA coatings process (Bastari et al., 2014). Even if there is a loss, the decrease is marginal since electrostatic interaction between negatively charged ciprofloxacin (Url-1) and positive adsorption part of hydroxyapatites reduces the release rate at pH 10 (Lee et al., 2009). This decrease may also be caused by newly formed nHA layers blocking the available pores (Bastari et

al., 2014) or decreasing water absorbency (Mahdavinia et al., 2019). Another reason for the decrease in the amount of drug released can be explained by the additional diffusion and mass transfer barrier produced by nHA layer affecting drug release rate.

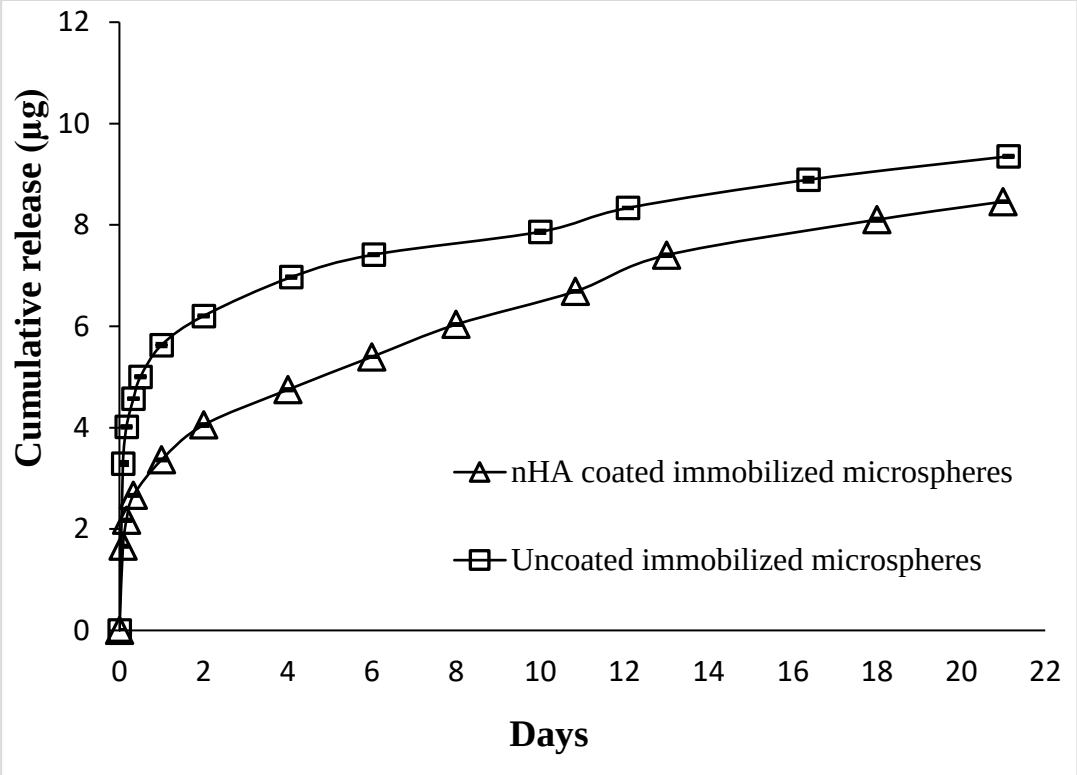

Figure 3.21 : Overall cumulative release of ciprofloxacin from nHA coated and uncoated immobilized microspheres.

Percentage drug release was examined to analyze the burst release and it was showed that 53.6 % of the loaded ciprofloxacin was released from the uncoated microspheres during 24 h while 31.9 % of the loaded drug was released from nHA coated microspheres (Figure 3.22). The decrease in burst release rate after the nHA coating was observed.

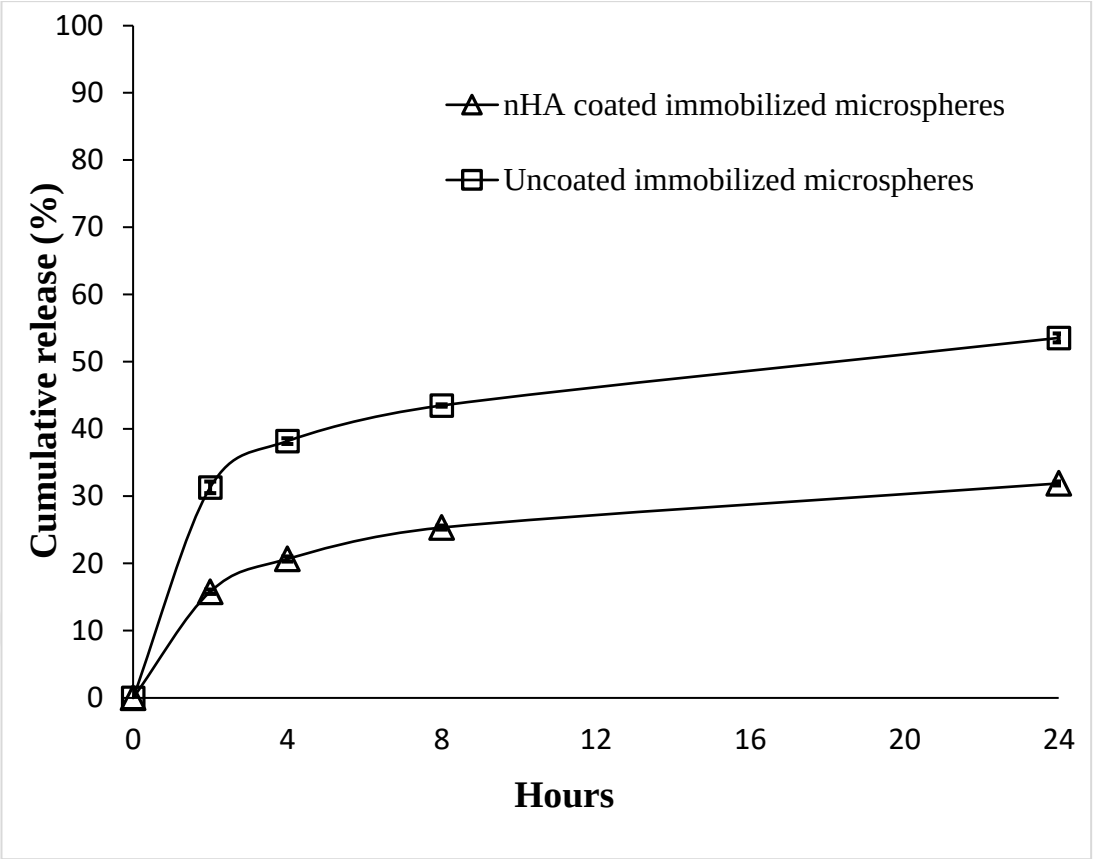

Figure 3.22 : Percentage cumulative release of ciprofloxacin from nHA coated and uncoated immobilized microspheres for 24 h.

As a result, it can be said that sustained drug release from nHA coated chitosan-microsphere modified Ti surfaces was successful.

4. CONCLUSIONS AND RECOMMENDATIONS

In this study, Ti surfaces were modified to prevent implant-associated infections and improve the tissue-implant integration. For this purpose, antibiotic loaded chitosan microspheres were prepared and immobilized on the Ti surface. Then, prepared Ti surfaces were coated with nano hydroxyapatite (nHA).

In the first part of the study, the size of microspheres was analyzed, and it was observed that microspheres with suitable size and size distribution were obtained at 500 rpm; their sizes were smaller and consequently they provide higher surface/volume ratio and their size distribution is was narrower leaning a more homogeneous coating. The microsphere-chitosan ratio (mg:µl) and amounts were found to be important for stable and homogeneous coating. The ratio of 5:50 (mg:µl) was chosen for 1.5 cm^2 Ti plate since the chitosan film was not fractured, and the microspheres were homogeneously distributed and not separated from the surface. Drug release studies were carried out and showed that chitosan film which provides the attachment of microsphere caused decreased drug release rate because it introduces an additional barrier. In the second part of the study, microsphere – chitosan modified Ti samples were coated with nHA and drug release studies were conducted with these samples. A slowdown of the drug release rate was observed after the nHA coating. This can be originated from the effect of nHA on the porous structure or water absorbency of the surface.

This dual-functional system can be functionalized further by loading different drugs or growth factors into microspheres and used to design effective implant material. In conclusion, antibiotic-loaded chitosan microspheres were attached on the Ti surface successfully and sustained drug release was observed from these surfaces.

REFERENCES

Adikwu, E., & Brambaifa, N. (2012). Ciprofloxacin Cardiotoxicity and Hepatotoxicity in Humans and Animals. *Pharmacology & Pharmacy*, *03*(02), 207–213. https://doi.org/10.4236/pp.2012.32028

Ahsan, S. M., Thomas, M., Reddy, K. K., Sooraparaju, S. G., Asthana, A., & Bhatnagar, I. (2018). Chitosan as biomaterial in drug delivery and tissue engineering. *International Journal of Biological Macromolecules*, *110*, 97–109. https://doi.org/10.1016/j.ijbiomac.2017.08.140

Bastari, K., Arshath, M., Ng, Z. H. M., Chia, J. H., Yow, Z. X. D., Sana, B., Tan, M. F. C., Lim, S., & Loo, S. C. J. (2014). A controlled release of antibiotics from calcium phosphate-coated poly(lactic-co-glycolic acid) particles and their in vitro efficacy against Staphylococcus aureus biofilm. *Journal of Materials Science: Materials in Medicine*, *25*(3), 747–757. https://doi.org/10.1007/s10856-013-5125-9

Campos, E. V. R., Oliveira, J. L., & Fraceto, L. F. (2017). Poly(ethylene glycol) and cyclodextrin-grafted chitosan: From methodologies to preparation and potential biotechnological applications. *Frontiers in Chemistry*, *5*(NOV), 1–15. https://doi.org/10.3389/fchem.2017.00093

Chen, Q., & Thouas, G. A. (2015). Metallic implant biomaterials. *Materials Science and Engineering R: Reports*, *87*, 1–57. https://doi.org/10.1016/j.mser.2014.10.001

Cuellar-Flores, M., Acosta-Torres, L. S., Martinez-Alvarez, O., Sanchez-Trocino, B., De La Fuente-Hernandez, J., Garcia-Garduno, R., & Garcia-Contreras, R. (2016). Effects of alkaline treatment for fibroblastic adhesion on titanium. *Dental Research Journal*, *13*(6), 473–477. https://doi.org/10.4103/1735-3327.197043

Dorozhkin, S. V. (2010). Nanosized and nanocrystalline calcium orthophosphates. *Acta Biomaterialia*, *6*(3), 715–734. https://doi.org/10.1016/j.actbio.2009.10.031

Elgadir, M. A., Uddin, M. S., Ferdosh, S., Adam, A., Chowdhury, A. J. K., & Sarker, M. Z. I. (2015). Impact of chitosan composites and chitosan nanoparticle composites on various drug delivery systems: A review. *Journal of Food and Drug Analysis*, *23*(4), 619–629. https://doi.org/10.1016/j.jfda.2014.10.008

Ferraris, S., & Spriano, S. (2016). Antibacterial titanium surfaces for medical implants. *Materials Science and Engineering C*, *61*, 965–978. https://doi.org/10.1016/j.msec.2015.12.062

Francolini, I., Vuotto, C., Piozzi, A., & Donelli, G. (2017). Antifouling and antimicrobial biomaterials: an overview. *Apmis*, *125*(4), 392–417.

https://doi.org/10.1111/apm.12675

Ghasemi-Mobarakeh, L., Kolahreez, D., Ramakrishna, S., & Williams, D. (2019). Key terminology in biomaterials and biocompatibility. *Current Opinion in Biomedical Engineering*, *10*, 45–50. https://doi.org/10.1016/j.cobme.2019.02.004

Gonçalves, V. L., Laranjeira, M. C. M., Fávere, V. T., & Pedrosa, R. C. (2005). Effect of crosslinking agents on chitosan microspheres in controlled release of diclofenac sodium. *Polímeros*, *15*(1), 6–12. https://doi.org/10.1590/s0104-14282005000100005

Grainger, D. W. (2013). All charged up about implanted biomaterials. *Nature Biotechnology*, *31*(6), 507–509. https://doi.org/10.1038/nbt.2600

Gulati, K., Ramakrishnan, S., Sinn, M., Atkins, G. J., Findlay, D. M., & Losic, D. (2012). Biocompatible polymer coating of titania nanotube arrays for improved drug elution and osteoblast adhesion. *Acta Biomaterialia*, *8*(1), 449–456. https://doi.org/10.1016/j.actbio.2011.09.004

Hetrick, E. M., & Schoenfisch, M. H. (2006). Reducing implant-related infections: Active release strategies. *Chemical Society Reviews*, *35*(9), 780–789. https://doi.org/10.1039/b515219b

Jayakumar, R., Menon, D., Manzoor, K., Nair, S. V., & Tamura, H. (2010). Biomedical applications of chitin and chitosan based nanomaterials - A short review. *Carbohydrate Polymers*, *82*(2), 227–232. https://doi.org/10.1016/j.carbpol.2010.04.074

Kaur, M., & Singh, K. (2019). Review on titanium and titanium based alloys as biomaterials for orthopaedic applications. *Materials Science and Engineering C*, *102*(February), 844–862. https://doi.org/10.1016/j.msec.2019.04.064

Kharbanda, O. P., Sharan, J., Koul, V., Dinda, A. K., Mishra, M., Gupta, G., & Singh, M. P. (2017). Tethering of 3-aminopropyltriethoxy silane films on medical grade V titanium alloy surface through self-assembled monolayers (SAMs) for biomedical applications. *Applied Surface Science*, *412*, 648–656. https://doi.org/10.1016/j.apsusc.2017.03.143

Kildeeva, N. R., Perminov, P. A., Vladimirov, L. V., Novikov, V. V., & Mikhailov, S. N. (2009). About mechanism of chitosan cross-linking with glutaraldehyde. *Russian Journal of Bioorganic Chemistry*, *35*(3), 360–369. https://doi.org/10.1134/S106816200903011X

Kim, H. W., Kim, H. E., & Salih, V. (2005). Stimulation of osteoblast responses to biomimetic nanocomposites of gelatin-hydroxyapatite for tissue engineering scaffolds. *Biomaterials*, *26*(25), 5221–5230. https://doi.org/10.1016/j.biomaterials.2005.01.047

Kong, L., Gao, Y., Lu, G., Gong, Y., Zhao, N., & Zhang, X. (2006). A study on the bioactivity of chitosan/nano-hydroxyapatite composite scaffolds for bone tissue engineering. *European Polymer Journal*, *42*(12), 3171–3179. https://doi.org/10.1016/j.eurpolymj.2006.08.009

Kurtz, I. S., & Schiffman, J. D. (2018). Current and emerging approaches to engineer antibacterial and antifouling electrospun nanofibers. *Materials*, *11*(7).

https://doi.org/10.3390/ma11071059

Lee, M., Li, W., Siu, R. K., Whang, J., Zhang, X., Soo, C., Ting, K., & Wu, B. M. (2009). Biomimetic apatite-coated alginate/chitosan microparticles as osteogenic protein carriers. *Biomaterials*, *30*(30), 6094–6101. https://doi.org/10.1016/j.biomaterials.2009.07.046

Li, C., Wang, J., Wang, Y., Gao, H., Wei, G., Huang, Y., Yu, H., Gan, Y., Wang, Y., Mei, L., Chen, H., Hu, H., Zhang, Z., & Jin, Y. (2019). Recent progress in drug delivery. *Acta Pharmaceutica Sinica B*, *9*(6), 1145–1162. https://doi.org/10.1016/j.apsb.2019.08.003

Li, D., Lu, X., Lin, H., Ren, F., & Leng, Y. (2013). Chitosan/bovine serum albumin co-micropatterns on functionalized titanium surfaces and their effects on osteoblasts. *Journal of Materials Science: Materials in Medicine*, *24*(2), 489–502. https://doi.org/10.1007/s10856-012-4810-4

Li, M., Wang, Y., Liu, Q., Li, Q., Cheng, Y., Zheng, Y., Xi, T., & Wei, S. (2013). In situ synthesis and biocompatibility of nano hydroxyapatite on pristine and chitosan functionalized graphene oxide. *Journal of Materials Chemistry B*, *1*(4), 475–484. https://doi.org/10.1039/c2tb00053a

Mahdavinia, G. R., Karimi, M. H., Soltaniniya, M., & Massoumi, B. (2019). In vitro evaluation of sustained ciprofloxacin release from κ-carrageenan-crosslinked chitosan/hydroxyapatite hydrogel nanocomposites. *International Journal of Biological Macromolecules*, *126*, 443–453. https://doi.org/10.1016/j.ijbiomac.2018.12.240

Mali, S. A., Nune, K. C., & Misra, R. D. K. (2016). Biomimetic nanostructured hydroxyapatite coatings on metallic implant materials. *Materials Technology*, *31*(13), 782–790. https://doi.org/10.1080/10667857.2016.1224609

Manivasagam, G., Dhinasekaran, D., & Rajamanickam, A. (2010). Biomedical Implants: Corrosion and its Prevention - A Review~!2009-12-22~!2010-01-20~!2010-05-25~! *Recent Patents on Corrosion Science*, *2*(1), 40–54. https://doi.org/10.2174/1877610801002010040

Moriarty, T. F., Poulsson, A. H. C., Rochford, E. T. J., & Richards, R. G. (2017). Bacterial adhesion and biomaterial surfaces. *Comprehensive Biomaterials II*, *4*, 101–129. https://doi.org/10.1016/B978-0-08-100691-7.00106-3

Nair, R., Reddy, B. H., Kumar, C. K. A., & Kumar, K. J. (2009). Application of chitosan microspheres as drug carriers: A review. *Journal of Pharmaceutical Sciences and Research*, *1*(2), 1–12.

Ni, J., Ling, H., Zhang, S., Wang, Z., Peng, Z., Benyshek, C., Zan, R., Miri, A. K., Li, Z., Zhang, X., Lee, J., Lee, K. J., Kim, H. J., Tebon, P., Hoffman, T., Dokmeci, M. R., Ashammakhi, N., Li, X., & Khademhosseini, A. (2019). Three-dimensional printing of metals for biomedical applications. *Materials Today Bio*, *3*(August). https://doi.org/10.1016/j.mtbio.2019.100024

Ong, J. L., & Chan, D. C. N. (2000). Hydroxyapatite and their use as coatings in

dental implants: A review. *Critical Reviews in Biomedical Engineering*, *28*(5–6), 667–707. https://doi.org/10.1615/CritRevBiomedEng.v28.i56.10

Reyes-Gasga, J., Martínez-Piñeiro, E. L., Rodríguez-Álvarez, G., Tiznado-Orozco, G. E., García-García, R., & Brès, E. F. (2013). XRD and FTIR crystallinity indices in sound human tooth enamel and synthetic hydroxyapatite. *Materials Science and Engineering C*, *33*(8), 4568–4574. https://doi.org/10.1016/j.msec.2013.07.014

Salah, T. A., Mohammad, A. M., Hassan, M. A., & El-Anadouli, B. E. (2014). Development of nano-hydroxyapatite/chitosan composite for cadmium ions removal in wastewater treatment. *Journal of the Taiwan Institute of Chemical Engineers*, *45*(4), 1571–1577. https://doi.org/10.1016/j.jtice.2013.10.008

Santos, A., Sinn Aw, M., Bariana, M., Kumeria, T., Wang, Y., & Losic, D. (2014). Drug-releasing implants: Current progress, challenges and perspectives. *Journal of Materials Chemistry B*, *2*(37), 6157–6182. https://doi.org/10.1039/c4tb00548a

Sharma, A., Sharma, A. K., Sharma, S., & Mishra, N. (2018). Oral Controlled Release Drug Delivery System : A Promising Approach for the Treatment of Ulcerative Colitis. *Journal of Chemical and Pharmaceutical Research*, *10*(1), 126–138.

Sharma, N., Purwar, N., & Gupta, P. C. (2015). Microspheres As Drug Carriers for Controlled Drug Delivery : a Review. *International Journal of Pharmaceutical Sciences and Research*, *6*(11), 4579–4587. https://doi.org/10.13040/IJPSR.0975-8232.6(11).4579-87

Sharma, P. C., Jain, A., Jain, S., Pahwa, R., & Yar, M. S. (2010). Ciprofloxacin: Review on developments in synthetic, analytical, and medicinal aspects. *Journal of Enzyme Inhibition and Medicinal Chemistry*, *25*(4), 577–589. https://doi.org/10.3109/14756360903373350

Son, G. H., Lee, B. J., & Cho, C. W. (2017). Mechanisms of drug release from advanced drug formulations such as polymeric-based drug-delivery systems and lipid nanoparticles. *Journal of Pharmaceutical Investigation*, *47*(4), 287–296. https://doi.org/10.1007/s40005-017-0320-1

Sopyan, I., Mel, M., Ramesh, S., & Khalid, K. A. (2007). Porous hydroxyapatite for artificial bone applications. *Science and Technology of Advanced Materials*, *8*(1–2), 116–123. https://doi.org/10.1016/j.stam.2006.11.017

Tsiourvas, D., Tsetsekou, A., Arkas, M., Diplas, S., & Mastrogianni, E. (2011). Covalent attachment of a bioactive hyperbranched polymeric layer to titanium surface for the biomimetic growth of calcium phosphates. *Journal of Materials Science: Materials in Medicine*, *22*(1), 85–96. https://doi.org/10.1007/s10856-010-4181-7

Williams, D. F. (2009). On the nature of biomaterials. *Biomaterials*, *30*(30), 5897–5909. https://doi.org/10.1016/j.biomaterials.2009.07.027

Zhe, Z., Zhang, S., Venkatraman, S. S., & Lei, S. (2011). Growth of hydroxyapatite coating on polymer microspheres. *Nanoscience and Nanotechnology Letters*, *3*(4), 472–476. https://doi.org/10.1166/nnl.2011.1204

Url-1 < https://pubchem.ncbi.nlm.nih.gov> date retrieved 04.06.2020

APPENDICES

APPENDIX A: Buffers

APPENDIX A

Phosphate Buffered Saline (0.01M) pH 7.4

0.2 g KCl

8 g NaCl

0.24 g KH_2PO_4

1.44 g Na_2HPO_4

are dissolved in 900 ml distilled water and then the volume of solution is adjusted to 1 l and buffer pH is adjusted to 7.4.

CURRICULUM VITAE

Name Surname **:Burcu Doymuş**

Place and Date of Birth **:Giresun, 10.10.1994**

E-Mail **:burcudoymus@gmail.com**

EDUCATION **:**

- **B.Sc.** **:** 2017, Isik University, Electric Electronic Faculty, Biomedical Engineering Department

PUBLICATIONS, PRESENTATIONS AND PATENTS ON THE THESIS:

- B. Doymus, Y. Ersan, F. N. Kok, S. Onder "Antimikrobiyal Özelliklerini Geliştirmek Üzere Titanyum Yüzeylerin Değiştirilmesi" 23. Biyomedikal Bilim ve Teknolojileri Sempozyumu (BIOMED 2018 -TR) (Poster Sunumu)
- B. Doymus, F. N. Kok, S. Onder "Modification of Titanium Surface for Bone Implant Applications" 24th International Biomedical Science and Technology Symposium (BIOMED 2019) (Poster Presentation)